FULL TITLE

Hybridization promotes asexual reproduction in *Caenorhabditis* nematodes

SHORT TITLE

Asexual reproduction in *Caenorhabditis*

AUTHORS

Piero Lamelza[1,2], Janet M. Young[3], Luke M. Noble[4,#a], Lews Caro[1,2], Arielle Isakharov[2], Meenakshi Palanisamy[2], Matthew V. Rockman[4], Harmit S. Malik[1,3,5], Michael Ailion[1,2]*

AFFILIATIONS

[1]Molecular and Cellular Biology Graduate Program, University of Washington, Seattle, WA, USA

[2]Department of Biochemistry, University of Washington, Seattle, WA 98195, USA

[3]Division of Basic Sciences, Fred Hutchinson Cancer Research Center, Seattle, WA 98109, USA

[4]Department of Biology and Center for Genomics & Systems Biology, New York University, New York, NY 10003, USA

[5]Howard Hughes Medical Institute, Fred Hutchinson Cancer Research Center, Seattle, WA 98109, USA

[#a]Current address: Institut de Biologie, École Normale Supérieure, Centre National de la Recherche Scientifique (CNRS) UMR 8197, Institut National de la Santé et de la Recherche Médicale (INSERM) U1024, Paris, France, F-75005

[*]Corresponding author: mailion@uw.edu

ABSTRACT

Although most unicellular organisms reproduce asexually, most multicellular eukaryotes are obligately sexual. This implies that there are strong barriers that prevent the origin or maintenance of asexuality arising from an obligately sexual ancestor. By studying rare asexual animal species we can gain a better understanding of the circumstances that facilitate their evolution from a sexual ancestor. Of the known asexual animal species, many originated by hybridization between two ancestral sexual species. The balance hypothesis predicts that genetic incompatibilities between the divergent genomes in hybrids can modify meiosis and facilitate asexual reproduction, but there are few instances where this has been shown. Here we report that hybridizing two sexual *Caenorhabditis* nematode species (*C. nouraguensis* females and *C. becei* males) alters the normal inheritance of the maternal and paternal genomes during the formation of hybrid zygotes. Most offspring of this interspecies cross die during embryogenesis, exhibiting inheritance of a diploid *C. nouraguensis* maternal genome and incomplete inheritance of *C. becei* paternal DNA. However, a small fraction of offspring develop into viable adults that can be either fertile or sterile. Fertile offspring are produced asexually by sperm-dependent parthenogenesis (also called gynogenesis or pseudogamy); these progeny inherit a diploid maternal genome but fail to inherit a paternal genome. Sterile offspring are hybrids that inherit both a diploid maternal genome and a haploid paternal genome. Whole-genome sequencing of individual viable worms shows that diploid maternal inheritance in both fertile and sterile offspring results from an altered meiosis in *C. nouraguensis* oocytes and the inheritance of two randomly selected homologous chromatids. We hypothesize that hybrid incompatibility between *C. nouraguensis* and *C. becei* modifies maternal and paternal genome inheritance and indirectly induces gynogenetic reproduction. This system can be used to dissect the molecular mechanisms by which hybrid incompatibilities can facilitate the emergence of asexual reproduction.

AUTHOR SUMMARY

Eukaryotes employ two major reproductive strategies: sexual and asexual reproduction. Both types of reproduction have distinct theoretical costs and benefits, and most unicellular eukaryotes can switch between both modes. However, most multicellular eukaryotes are obligately sexual, implying that there are barriers to the evolution of asexuality from a sexual ancestor. Of the few asexual animal species, many are hybrids of two ancestral sexual species, suggesting that novel genetic interactions in hybrids facilitate the evolution of asexuality. One model suggests that genetic incompatibilities between divergent genomes in hybrids can modify female meiosis and paternal genome inheritance to facilitate asexual reproduction. While studying interspecies hybridizations of *Caenorhabditis* nematodes, we found that crossing two sexual species (*C. nouraguensis* and *C. becei*) disrupts female meiosis and paternal genome inheritance. Most offspring die during embryogenesis, but on rare occasions develop into viable and fertile adults that are produced asexually. This asexual reproduction involves the unusual production of eggs carrying two sets of maternal chromosomes and the loss of the paternal set of chromosomes. We hypothesize that genetic incompatibility between these two species disrupts maternal and paternal genome inheritance. This interspecies hybridization may serve as a model to study how genetic incompatibilities facilitate the emergence of asexuality.

Keywords: gynogenesis, pseudogamy, sperm-dependent parthenogenesis, asexual, *Caenorhabditis*, hybrid, diploid egg, paternal genome loss, balance hypothesis, automixis, central fusion, large X-effect, single-worm sequencing

INTRODUCTION

Sex is the most common form of reproduction in multicellular eukaryotes. In sex, diploid females and males generate haploid eggs and sperm that fuse to produce diploid offspring. Sex has theoretical benefits that may explain its prevalence. Namely, recombination during meiosis generates genotypic diversity that can be used to adapt to changing environments or purge deleterious alleles [1].

Despite the predicted advantages of sex, it also has theoretical costs, such as the need to find a mate and the production of offspring that inherit only half of an individual's genome [2,3]. By contrast, females of asexual species independently generate their own offspring and pass on their entire genome. Consistent with sex being costly, most unicellular organisms reproduce by either obligate or facultative asexuality [4,5], which involves being able to reproduce either sexually or asexually as conditions dictate. However, because obligate sex is the predominant form of reproduction in multicellular organisms [6], it is likely there are strong barriers that prevent the origin of asexuality from a sexual ancestor or its persistence [7]. By studying rare cases of asexual animal species, we can better understand the circumstances that facilitate the evolution of asexual reproduction.

Here we focus on two key aspects of how asexuality evolves from sexually reproducing organisms: diploid maternal inheritance and paternal genome loss. In contrast to sexual females that produce haploid eggs, asexual females produce diploid eggs that either develop independently of sperm fertilization, known as parthenogenesis [8], or require fertilization but fail to inherit the paternal genome, known as sperm-dependent parthenogenesis, gynogenesis, or pseudogamy [9]. Thus, understanding how egg production can be modified to result in diploid maternal inheritance and how the paternal genome is lost in gynogenetic reproduction should provide insight into how asexuality can arise.

95 Interestingly, many asexual animal species are hybrids of two ancestral sexually
96 reproducing species, suggesting that hybridization may play a role in the generation of asexual
97 species. However, hybridization is typically accompanied by deleterious incompatibilities between
98 the two divergent genomes. For example, hybrid incompatibilities are known to disrupt
99 gametogenesis and cause sterility [10,11], or perturb paternal genome replication and inheritance
100 and cause aneuploidy and lethality [12–14]. One model of how hybridization might lead to
101 asexuality is known as the "balance hypothesis." This model posits that in asexual hybrid species,
102 interspecies incompatibilities disrupt female meiosis enough to produce diploid eggs, but do not
103 significantly reduce the fertility or viability of hybrids [15,16]. Other interspecies incompatibilities,
104 such as incompatibility between components of the maternal egg cytoplasm and the paternal DNA
105 [12,14], may also facilitate paternal genome loss during gynogenetic reproduction. In support of
106 this possibility, the females of many gynogenetic species hybridize with males of a different
107 species [9,17]. Thus, incompatibilities between two species that alter meiosis and the fidelity of
108 paternal genome inheritance may actually in combination facilitate the generation of asexually-
109 produced viable progeny, even though such incompatibilities on their own would be deleterious
110 and lead to sterility or lethality.
111 In support of the balance hypothesis, there is good evidence that genetic incompatibilities
112 facilitate diploid maternal inheritance in the hybrid parthenogenetic lizard *Aspidoscelis*
113 *neomexicana* [18]. In most *A. neomexicana* female oocytes, the divergent homologous
114 chromosomes fail to properly pair, resulting in arrest during meiotic prophase. However, instead of
115 these hybrid females being sterile, a small number of oocytes duplicate their genomes and
116 become tetraploid. Pairing and recombination in these tetraploid oocytes occur between
117 genetically identical chromosomes, allowing these oocytes to progress through meiosis and
118 generate diploid eggs that develop independently of fertilization.

It is unclear how often interspecies incompatibilities facilitate asexual reproduction, and the mechanisms that allow such hybrids to be viable and fertile remain largely unknown. We looked for examples of asexual reproduction in interspecies crosses within the genus of *Caenorhabditis* nematodes. Here we report that a cross between two sexual *Caenorhabditis* species (*C. nouraguensis* and *C. becei)* results in most offspring dying during embryogenesis, but also rare viable progeny that are asexually produced. We hypothesize that genetic incompatibility between these two *Caenorhabditis* species facilitates diploid maternal inheritance and paternal genome loss. Both processes usually result in aneuploidy that leads to sterility or death of hybrid embryos, but on rare occasions can result in production of viable offspring by gynogenetic reproduction. The hybridization between these two *Caenorhabditis* species might serve as an excellent cellular and genetic model to study how interspecies incompatibilities can modify normal sexual reproduction to facilitate the evolution of asexuality.

131 **RESULTS**

132 **Reciprocal *C. nouraguensis* x *C. becei* crosses exhibit distinct F1 embryonic lethal**
133 **phenotypes**

134 *C. nouraguensis* and *C. becei* are obligately outcrossing sister species consisting of female
135 and male individuals (Fig 1A). We initially studied the hybridization of *C. nouraguensis* strain
136 JU1825 with *C. becei* strain QG711. The mating of individuals within the same strain results in a
137 high proportion of viable progeny (91-99% viability, Fig S1A, Videos S1 and S2). However, mating
138 *C. becei* females (QG711) to *C. nouraguensis* males (JU1825) results in 100% embryonic death
139 with a stereotypical arrest at approximately the 32-cell stage (Fig 1B, Video S3). In the reciprocal
140 cross between *C. nouraguensis* females (JU1825) and *C. becei* males (QG711), most F1 embryos
141 also die (~99.9%), but some embryos arrest early in development (approximately 1-4 cell stage)
142 whereas some arrest at later stages (approximately 44-87 cell stage) (Video S4). From the cross of
143 *C. nouraguensis* females (JU1825) and *C. becei* males (QG711), approximately 0.1% of F1
144 progeny survived and became viable adults (Fig 1B). Fecundity of *C. nouraguensis* females
145 crossed to *C. becei* males was similar to *C. nouraguensis* females in intraspecific crosses on the
146 first day of egg-laying but was mildly reduced on the second and third days of egg-laying (Fig
147 S1B), consistent with possible deleterious effects of interspecific sperm [19].

148

149 **Crossing *C. nouraguensis* females to *C. becei* males results in rare asexually-produced**
150 **progeny**

151 Interestingly, a small fraction of F1 progeny from *C. nouraguensis* female x *C. becei* male
152 crosses develop into viable adults. Such viable progeny were found using three different *C.*
153 *nouraguensis* strains and two *C. becei* strains (Fig S2), indicating that the production of viable
154 progeny is a general feature of *C. nouraguensis* female x *C. becei* male crosses. By contrast, no
155 surviving F1 were found in the reciprocal *C. becei* female x *C. nouraguensis* male crosses or

156 crosses between *C. nouraguensis* females and males of other closely related *Caenorhabditis*
157 species (Fig 1B and Fig S2). Thus, production of viable F1 progeny is specific to the *C.*
158 *nouraguensis* female x *C. becei* male cross. We tested the fertility of each viable F1 animal and
159 found that ~2/3 of F1 were sterile and ~1/3 were fertile (JU1825 x QG711: 18 sterile, 8 fertile;
160 NIC54 x QG711: 27 sterile, 10 fertile) (Fig 1D).

161 We next tested if the rare viable F1 were indeed interspecies hybrids. We genotyped each
162 F1 at one of two autosomal loci using PCR-restriction digest assays that distinguish between *C.*
163 *nouraguensis* and *C. becei* alleles (Fig 1C). We found that about two-thirds of viable F1 inherited
164 both parental alleles and therefore are genetic hybrids (JU1825 x QG711: 17/26 F1; NIC54 x
165 QG711: 26/37 F1). However, to our surprise, we found that the remaining viable F1 adults carry
166 only the maternal *C. nouraguensis* allele and no paternal *C. becei* allele (JU1825 x QG711: 9/26
167 F1; NIC54 x QG711: 11/37 F1) (Fig 1D). Interestingly, all fertile F1 had only the maternal *C.*
168 *nouraguensis* allele and not the paternal *C. becei* allele, while all but two sterile F1 had a hybrid
169 genotype with alleles from both parents. We observed a similar correlation between genotype and
170 fertility among rare viable F1 animals when a different paternal *C. becei* strain was used (Fig S3).

171 Interspecies hybrids are often sterile [10], but it was surprising to find fertile F1 that inherited
172 only maternal *C. nouraguensis* DNA. These fertile F1 behave like *C. nouraguensis* when
173 backcrossed to either parental species. Backcrossing fertile F1 to *C. nouraguensis* results in many
174 viable F2 progeny that develop to adulthood. By contrast, backcrossing fertile F1 to *C. becei*
175 results in almost all F2 dying during embryogenesis other than the few rare viable F2 progeny in
176 crosses to *C. becei* males (as in the original interspecies cross). Thus, it appears that interspecies
177 hybridization between *C. nouraguensis* females and *C. becei* males produces a low frequency of
178 fertile F1 that carry only maternal *C. nouraguensis* DNA and thus are produced asexually.

179 One way *C. nouraguensis* females might produce fertile F1 progeny with a maternal
180 genotype would be to generate sperm and reproduce as hermaphrodites at a low frequency. To

181 test this possibility, we monitored 60 virgin females from two *C. nouraguensis* strains (JU1825 and
182 NIC59) and two *C. becei* strains (QG704 and QG711) for five days but failed to find any progeny.
183 Thus, production of fertile F1 is not due to cryptic hermaphroditism but requires mating to *C. becei*
184 males. We conclude that fertile F1 are the result of gynogenetic reproduction in which *C.*
185 *nouraguensis* oocytes require fertilization by *C. becei* sperm to initiate development, but do not
186 inherit the paternal *C. becei* genome.
187

188 **Asexually-produced F1 females are diploid**

189 How do the fertile F1 compensate for the lack of a paternal haploid genome? We presumed
190 that the autosomes of the fertile F1 had to be at least diploid for viability because haploid *C.*
191 *elegans* individuals die during embryogenesis [20], and all well-studied *Caenorhabditis* species
192 have five diploid autosomes and an X chromosome that is either diploid (females) or haploid
193 (males) [21–23].

194 We determined the ploidy of fertile F1 females by counting the number of chromosomes in
195 their oocytes. In *C. elegans*, the female germline produces oocytes containing chromosomes that
196 have undergone prophase of meiosis I (DNA replication and recombination) but have yet to
197 undergo the two meiotic divisions. The oocyte contains six bivalents, each of which is composed of
198 a pair of homologous chromosomes and their sister chromatids held together by a combination of
199 recombination and sister chromatid cohesion (Fig 2A). Therefore, diploid individuals have six
200 bivalents in their oocytes, which appear as six distinct DAPI-staining bodies (Fig 2B). In *C.*
201 *elegans*, meiotic recombination occurs only once per homologous set of chromosomes [24]. Thus,
202 a triploid individual will have two homologous chromosomes that recombine and form a bivalent as
203 well as a non-recombinant homolog as a univalent. Therefore, triploid individuals have six bivalents
204 and six univalents in mature oocytes, which appear as twelve DAPI-staining bodies (Fig 2B) [25].

205 We crossed *C. nouraguensis* (JU1825) females to *C. becei* (QG711) males, collected fertile
206 F1 females and dissected and stained their germlines with DAPI. As controls, we examined the
207 germlines of JU1825 and QG711 females after mating with conspecific males. Both parental
208 species mostly have six DAPI-staining bodies, consistent with six diploid chromosomes (like *C.*
209 *elegans*). Most fertile F1 females also have six DAPI-staining bodies, indicating they are diploid
210 (Fig 2C and Fig S4).
211

212 **Asexually-produced F1 inherit two random homologous chromatids from each maternal *C.***
213 ***nouraguensis* bivalent**

214 There are three mechanisms by which the fertile F1 animals could result from diploid
215 maternal inheritance. They could inherit two chromatids from each maternal bivalent in a *C.*
216 *nouraguensis* oocyte, inherit one chromatid from each bivalent and undergo genome-wide
217 diploidization by endoreplication, or inherit the original two maternal chromatids by producing
218 diploid eggs by mitosis (apomixis). To distinguish between these possibilities, we used whole-
219 genome sequencing of individual worms to determine the genetic identity of the chromatids
220 inherited by fertile F1 individuals.

221 All four of the chromatids within a bivalent are genetically distinct; of the six possible ways of
222 combining two chromatids, four have distinct chromosomal genotypes and two are
223 indistinguishable by Illumina whole-genome sequencing (Fig 3A, 3B and Fig S5A). Thus, the
224 genotype of the fertile F1 can indicate which two chromatids were inherited. Because
225 recombination in *Caenorhabditis* species occurs predominantly on chromosome arms [26,27],
226 inheriting two sister chromatids would usually result in homozygosity in the centers of
227 chromosomes and heterozygosity on one of the arms, whereas inheriting two homologous
228 chromatids would result in heterozygosity in the center of each chromosome (Fig 3B). By contrast,

229 endoreplication of single chromatids would lead to homozygosity along all chromosomes, and
230 apomixis would lead to heterozygosity along all chromosomes (Fig S6).

231 We first crossed two genetically distinct *C. nouraguensis* strains, NIC59 and JU1825, to
232 generate heterozygous *C. nouraguensis* (NIC59/JU1825) females, which we then crossed to *C.*
233 *becei* (QG711) males. We collected eleven fertile F1 and performed whole-genome amplification
234 and sequencing of each one (Fig 3A). We determined the genotype of each fertile individual's
235 chromosomes by calculating average NIC59 SNP frequencies in 50-kb windows across their
236 genome (see Materials and Methods for details). An approximately 0.50 NIC59 allele frequency
237 was inferred as heterozygosity (NIC59/JU1825), whereas an approximately 1.0 or 0.0 NIC59 allele
238 frequency was inferred as homozygous NIC59 or JU1825, respectively. This experiment also
239 allowed us to determine whether fertile F1 inherit only maternal *C. nouraguensis* DNA or whether
240 some paternal *C. becei* DNA is also present.

241 We found that nearly 100% of each fertile F1's reads map to the *C. nouraguensis* genome
242 assembly; only a small percentage (0.1-0.2%) map to the *C. becei* genome assembly (Table S1
243 and Fig S7). These results resemble our controls that contain only *C. nouraguensis* DNA (samples:
244 F1_NIC59_JU1825 and NIC59plusJU1825, Table S1 and Fig S7). Therefore, our sequencing
245 results confirm that fertile F1 inherit only maternal *C. nouraguensis* DNA. Strikingly, whole-
246 chromosome genotyping data shows that the fertile F1 always inherited two homologous
247 chromatids from each maternal bivalent (Fig 3C, Fig S5 and Fig S7). Combining chromosome
248 genotypes from the fertile F1 indicates that two randomly selected homologous chromatids were
249 inherited (Fig 3D). Based on these findings, we can rule out endoreplication and apomixis, or a
250 failure of the second meiotic division that would result in inheritance of two sister chromatids.
251 Instead, we conclude that diploid, asexually-produced F1 inherit two homologous chromatids from
252 each maternal bivalent in *C. nouraguensis* oocytes.

253

254 **Sterile F1 inherit a diploid *C. nouraguensis* genome and a haploid *C. becei* genome**

255 Having established that fertile asexually-produced F1 adults inherit only a diploid maternal
256 genome, we next examined the genome-wide inheritance pattern in sterile hybrid F1 adults. We
257 performed whole-genome sequencing of ten sterile F1 adults derived from the same interspecies
258 crosses mentioned in the previous section (Fig 3A).

259 Surprisingly, five of the sterile F1 appear to be triploid hybrids that inherited a diploid *C.*
260 *nouraguensis* maternal genome and a haploid *C. becei* paternal genome (females F1_6, F1_12,
261 F1_20; males F1_17 and F1_21, Table S1). In these individuals, the normalized coverage of *C.*
262 *nouraguensis* autosomes was approximately double that of the *C. becei* autosomes (Fig 4A).
263 Furthermore, genotyping of the *C. nouraguensis* chromosomes revealed that these individuals
264 inherited two homologous chromatids from each maternal *C. nouraguensis* bivalent, just like the
265 fertile F1 (Fig 4B and Fig S7). Three other sterile F1 males are also hybrids that inherited two
266 homologous chromatids from each maternal bivalent. However, they are unlikely to be true, full
267 triploids because the normalized coverage of the *C. becei* autosomes is considerably less than half
268 that of the *C. nouraguensis* autosomes (males: F1_10, F1_16 and F1_23, Fig 4A). Instead, we
269 hypothesize that the reduced coverage of the *C. becei* genome results from mosaicism, in which
270 only a subset of cells in these individuals contain the paternal *C. becei* DNA. The *C. becei*
271 autosomes within each individual hybrid mosaic exhibit similar levels of coverage (except perhaps
272 Chr. V of F1_16), suggesting that most hybrid cells within these individuals have a complete
273 haploid copy of the *C. becei* autosomal genome (diploid-triploid mosaic hybrids) (Fig 4A). By
274 scoring viable animals, we may be selecting against individuals that have partial losses of the
275 paternal genome since such animals would be aneuploid in at least some cells. Alternatively, the
276 cellular mechanism of paternal genome loss may lead to loss of the complete paternal set of
277 chromosomes.

278 Combining maternal chromosome genotypes from the sterile F1 indicates that two randomly
279 selected homologous chromatids were inherited (Fig 4C and Fig S5C). Additionally, the combined
280 data on maternal genotype frequencies from both sterile and fertile F1 also indicate random
281 homologous chromatid inheritance (Fig 4D and Fig S5C). These results show that the fertile and
282 sterile F1 share the same mechanism of diploid maternal inheritance and are distinguished by
283 whether they inherit the haploid *C. becei* genome.
284

285 **The *C. becei* X-chromosome is toxic to F1 hybrids**

286 In *Caenorhabditis*, males are hemizygous for the X-chromosome (XO) and produce haploid
287 sperm that carry either a single X or no X. Therefore, roughly half of the F1 are expected to inherit
288 the paternal *C. becei* X-chromosome. However, though the sterile F1 inherited *C. becei*
289 autosomes, none inherited the *C. becei* X-chromosome (Fig S7). We collected additional viable F1
290 hybrids from the interspecies cross and determined whether any inherited the *C. becei* X-
291 chromosome by PCR genotyping of two indel polymorphisms, one X-linked and one autosomal,
292 that distinguish between *C. nouraguensis* and *C. becei* sequences (Fig 5A). We found that none of
293 the F1 inherited the *C. becei* X-chromosome (Fig 5B), regardless of whether they were autosomal
294 hybrids (22 females and 12 males) or had a maternal genotype (10 females).

295 Our failure to find any viable F1 carrying a *C. becei* X-chromosome suggests that it is toxic
296 to F1 hybrids. Alternatively, this pattern could reflect an unusual segregation pattern specifically
297 involving the X chromosome in hybrids. To distinguish between these possibilities, we PCR
298 genotyped dead F1 embryos from the same interspecies cross. Consistent with the expected
299 inheritance of the X-chromosome from males, we found that 17 of 34 (50%) dead F1 embryos
300 inherited both the *C. becei* paternal X-chromosome and the *C. nouraguensis* maternal X-
301 chromosome, whereas 16 of 34 (47%) inherited only the maternal *C. nouraguensis* X-chromosome
302 (Fig 5B). One dead F1 embryo possessed only a paternal *C. becei* genotype, suggesting that it lost

303 the maternal *C. nouraguensis* X-chromosome. Because dead F1 embryos can inherit the *C. becei*
304 X-chromosome but viable F1 animals do not, we conclude that the *C. becei* X-chromosome is toxic
305 to F1 hybrids. Previous work has described the "large X-effect" on hybrid inviability and sterility
306 [10]. We hypothesize that a dominant incompatibility involving one or more loci on the *C. becei* X
307 chromosome underlies its toxic effect on hybrids with *C. nouraguensis*.
308

309 **Dead F1 embryos have unusual maternal and paternal inheritance**

310 To determine whether the unusual patterns of maternal and paternal inheritance seen in
311 viable F1 also occur in the dead F1 embryos in the interspecies cross, we PCR genotyped the
312 same dead F1 embryos described above at an autosomal indel polymorphism that distinguishes
313 the two species (Fig 5C). We found that 27 of the 35 dead F1 embryos (77%) had a heterozygous
314 *C. nouraguensis*/*C. becei* genotype while eight (22%) had an only-maternal *C. nouraguensis*
315 genotype (Fig 5C). These data suggest that although most embryos inherited both maternal and
316 paternal DNA, a significant fraction failed to inherit paternal *C. becei* DNA for this marker.
317 However, given that only a single marker was scored, it is possible that these embryos inherited
318 paternal DNA for other chromosomes and were aneuploid. Aneuploidy caused by incomplete loss
319 of the paternal genome may contribute to death of embryos.

320 To determine whether dead F1 embryos also inherit two homologous *C. nouraguensis*
321 chromatids from each maternal bivalent, we PCR genotyped them at an autosomal indel
322 polymorphism in the center of chromosome I that distinguishes NIC59 and JU1825 alleles. We
323 found that 34 of 36 dead F1 embryos had a heterozygous NIC59/JU1825 genotype, whereas one
324 embryo had a JU1825 genotype and one embryo had a NIC59 genotype (Fig 5D). These data
325 suggest that very few embryos are derived from a canonical female meiosis in which a haploid
326 maternal complement is inherited. Instead, most embryos appear to have inherited two
327 homologous chromatids from an aberrant female meiosis.

328 To better understand how female meiosis is modified so that two homologous chromatids
329 are inherited, we quantified the number of polar bodies found in F1 embryos, of which the vast
330 majority are expected to die. If most *C. nouraguensis* oocytes fertilized by *C. becei* sperm have
331 aberrant meiotic segregations that result in the inheritance of two homologous chromatids, we
332 would predict that fewer than two polar bodies are formed. We DAPI stained F1 embryos derived
333 from crossing *C. nouraguensis* (NIC59) females to *C. becei* (QG711) males. As a control, we
334 stained embryos derived from intraspecies NIC59 crosses. As expected, NIC59 embryos almost
335 always have two polar bodies whose morphology and size appear similar across individuals (Fig
336 5E and 5I). Interestingly, we found that 2/90 NIC59 embryos had only one polar body (Fig 5F and
337 5I), suggesting that abnormal meiosis can occur at a low frequency in intraspecies crosses. By
338 contrast, approximately half of the hybrid embryos have only one polar body (52/102), suggesting
339 that one of the two female meiotic divisions has failed (Fig 5G-I). The polar bodies in hybrid
340 embryos can also appear abnormal in their morphology (Fig 5I). Together with our genotyping
341 data, these observations indicate that meiotic segregations are frequently perturbed in *C.*
342 *nouraguensis* females mated to *C. becei* males.
343

344 **Hybrid embryos inherit sperm centrioles and DNA, but exhibit mitotic defects**

345 During fertilization in *Caenorhabditis,* the sperm deposits centrioles and a condensed
346 paternal genome into the egg where it forms a pronucleus (Fig 6A). The paternal pronucleus then
347 decondenses and migrates to join the maternal pronucleus for the first mitotic division (Fig 6B-E)
348 [28]. In obligately gynogenetic species, the paternal genome can be lost by remaining condensed
349 during the first few mitotic divisions of the zygote rather than being replicated and segregated
350 properly [29,30]. To determine how the paternal genome behaves in hybrid embryos, we stained
351 *C. nouraguensis* x *C. becei* F1 hybrid embryos with DAPI (staining DNA) and antibodies to α-
352 tubulin (staining spindles) and γ-tubulin (staining centrosomes). We found that hybrid embryos

353 always have centrioles and a paternal genome derived from the sperm as is normal in
354 *Caenorhabditis*, but in a small fraction of animals, the centrioles are abnormally dissociated from
355 the male pronucleus (Fig 6M and 6Q). We consistently observed both paternal and maternal
356 pronuclei decondensing and meeting (Fig 6I-L and 6Q). Thus, unlike obligate gynogenetic species,
357 there is not frequent failure of the paternal genome to decondense in these hybrid embryos.
358 However, it is possible that the paternal genome fails to decondense at a low frequency and that
359 those embryos are the ones that exhibit clean paternal genome loss and become fertile adults.
360 We also observed later stages of hybrid embryogenesis from metaphase of the first mitosis
361 to the four-cell stage. We found that a fraction of hybrid embryos exhibit DNA that is not properly
362 aligned on the mitotic spindle (Fig 6N and 6Q), lagging DNA during or after anaphase (Fig 6O and
363 6Q), and probable micronuclei during interphase (Fig 6P and 6Q). Although it is unclear whether
364 the aberrant DNA is maternal or paternal, these data are consistent with some paternal genome
365 loss at later embryonic stages.
366

367 **Diploid maternal inheritance occurs occasionally in *C. nouraguensis* intraspecies crosses**

368 Because we observed a low frequency of embryos with a single polar body in normal
369 intraspecies *C. nouraguensis* crosses (2/90, Fig 5F and 5I), we wondered whether diploid maternal
370 inheritance could occur at low frequency within *C. nouraguensis* independently of interspecies
371 hybridization. To more sensitively and directly assay for diploid maternal inheritance within *C.*
372 *nouraguensis*, we designed an experiment in which *C. nouraguensis* sperm can fertilize *C.*
373 *nouraguensis* oocytes but do not contribute the paternal genome. In this scenario, a canonical
374 female meiosis would result in haploid maternal embryos that would fail to develop into viable
375 adults [20]. However, if *C. nouraguensis* oocytes inherit a diploid maternal genome, they could
376 complete embryogenesis and develop into viable adults.

377 We blocked the inheritance of the haploid sperm genome using UV irradiation to damage
378 and inactivate the sperm genome while still allowing for fertilization and development of the
379 maternal haploid embryo [31,32]. We exposed NIC59 and JU1825 adult males to a high dose of
380 shortwave UV radiation and then crossed them to non-irradiated JU1825 or NIC59 adult virgin
381 females, respectively. We then screened for and PCR genotyped viable progeny at several
382 autosomal loci to determine whether they inherited both maternal and paternal DNA (heterozygous
383 NIC59/JU1825) or just maternal DNA (Fig 7A).

384 From a cross of JU1825 females to NIC59 UV-irradiated males, only seven out of
385 approximately 18,000 embryos survived to adulthood. Upon PCR genotyping a chromosome I
386 indel polymorphism, we found that four of these seven individuals had a heterozygous
387 NIC59/JU1825 genotype and therefore inherited both maternal and paternal alleles at this locus.
388 We presume these animals represent rare cases in which the sperm genome was not destroyed.
389 However, three females inherited only the maternal JU1825 allele (Fig 7B). We PCR genotyped
390 these females at two other unlinked autosomal indel polymorphisms. All had a maternal JU1825
391 genotype at all three loci, suggesting that they inherited only the maternal genome and were
392 asexually-produced (Fig 7C). We performed similar experiments with NIC59 females and UV-
393 irradiated JU1825 males. Only two out of roughly 7,000 progeny survived to adulthood. These two
394 females had only-maternal NIC59 genotypes at all three autosomal loci (Fig 7B and 7C). We
395 performed additional UV-experiments to better quantify the frequency of gynogenetically-produced
396 offspring. In total, we found that gynogenetically-produced offspring occur at a rate of ~0.01% in
397 JU1825 female x NIC59 male UV crosses and ~0.1% in NIC59 female x JU1825 male UV crosses.
398 Interestingly, each cross had a single gynogenetically-produced male (Fig 7D).

399 We then determined the ploidy of the gynogenetically-produced females from the UV
400 experiments by counting the number of DAPI-staining bodies in their -1 oocytes. We found that
401 almost all had six DAPI-staining bodies, indicating that they result from diploid maternal inheritance

402 (Fig 7E). The genotyping and DAPI staining data together indicate that diploid maternal inheritance
403 in *C. nouraguensis* oocytes does not require fertilization by *C. becei* sperm and can occur even in
404 intraspecies crosses, at least when the males are sterilized by UV.

405 A caveat to the UV experiments is that they may not be indicative of what occurs during
406 normal non-irradiated intraspecies crosses. For instance, diploid maternal inheritance could be
407 artificially induced by fertilization with UV-damaged sperm. To determine whether female meiosis is
408 perturbed when oocytes are fertilized by UV-irradiated sperm, we stained embryos derived from
409 JU1825 female x NIC59 male UV crosses. We found that the embryos we scored all exhibited two
410 superficially normal polar bodies, much like the non-UV control (Fig 7F-H). This result suggests
411 that female meiosis is usually normal when an oocyte is fertilized by UV-damaged sperm.
412 Furthermore, PCR genotyping of dead embryos derived from crossing heterozygous
413 NIC59/JU1825 females to NIC59 UV-irradiated males is consistent with haploid maternal
414 inheritance and destruction of the paternal NIC59 genome (Fig S8). Therefore, our data suggest
415 that female meiosis is not generally perturbed by fertilization with UV-irradiated sperm, and that the
416 diploid maternal inheritance seen in intraspecies crosses is not an artificial byproduct of a grossly
417 disrupted meiosis. In support of this, we observe occasional embryos derived from normal
418 intraspecies crosses with only a single polar body (Fig 5F and 5I, and Fig 7H), consistent with
419 diploid maternal inheritance occurring in *C. nouraguensis* at a low frequency independently of UV-
420 irradiation.

421 **DISCUSSION**

422 In this study we investigated the hybridization of two sexual *Caenorhabditis* species, *C.*
423 *nouraguensis* and *C. becei*. We found that rare viable offspring are produced in the cross of *C.*
424 *nouraguensis* females to *C. becei* males. About one-third of the viable offspring are fertile and
425 result from a combination of diploid maternal inheritance and paternal genome loss, two traits that
426 define asexual gynogenetic reproduction. The remaining viable offspring are sterile and possess a
427 diploid maternal *C. nouraguensis* genome and a haploid paternal *C. becei* genome. Furthermore,
428 dead hybrid embryos also inherit two homologous maternal chromosomes, like the viable offspring,
429 indicating that diploid maternal inheritance is a general feature of this cross. Finally, we found that
430 diploid maternal inheritance can also occur at a low frequency in intraspecies *C. nouraguensis*
431 crosses, as revealed by UV-irradiation of males. These data suggest that meiosis may be
432 inherently fragile in *C. nouraguensis* oocytes and primed for diploid maternal inheritance. However,
433 the frequency of diploid maternal inheritance is drastically increased when these oocytes are
434 fertilized by *C. becei* sperm, suggesting that unknown factors present in *C. becei* sperm somehow
435 alter *C. nouraguensis* female meiosis.

436

437 **Mechanism of diploid maternal inheritance**

438 We found that diploid maternal inheritance in fertile and sterile offspring almost always
439 results from inheriting two randomly selected homologous chromatids from each maternal bivalent
440 in the oocyte. We hypothesize that this diploid maternal inheritance reflects a stereotypical
441 segregation mechanism that is a slight modification of canonical meiotic divisions (Fig 8A).

442 We propose that gynogenetic development in *C. nouraguensis* results from an alteration of
443 the first meiotic division followed by a normal second meiotic division. In our model (Fig 8B),
444 homologous chromosomes segregate normally at anaphase I, but instead of segregating one set
445 of homologs into the first polar body, both sets are retained in the oocyte. Both half-bivalents within

446 the oocyte then randomly segregate sister chromatids at anaphase II. One chromatid segregates
447 into a polar body while the other is retained in the oocyte. Thus, the oocyte inherits two randomly
448 selected homologous chromatids from each bivalent. This model suggests that diploid maternal
449 inheritance could result from a modification of female meiosis such as failure of cytokinesis after
450 anaphase I. There is cytological evidence that incomplete anaphase I and a failure of cytokinesis
451 generates diploid eggs in *Daphnia pulex*, which undergoes obligate parthenogenesis [33].

452 Importantly, our model predicts the formation of only one polar body (Fig 8B). Approximately
453 half of the dead hybrid embryos have only one polar body (Fig 5G and 5I). Combined with the fact
454 that dead hybrid embryos also inherit two maternal homologs (Fig 5D), our data suggest these
455 embryos also undergo the same mechanism of diploid maternal inheritance as the viable progeny.
456 But if almost all embryos have diploid maternal inheritance (Fig 5D), why do approximately half still
457 have two polar bodies? One possibility is that the two half-bivalents formed by the incomplete first
458 meiotic division are sometimes segregated on the same spindle at meiosis II, resulting in one polar
459 body, but are sometimes segregated on separate spindles for meiosis II, resulting in two polar
460 bodies.

461 How might meiosis I be disrupted to produce diploid maternal inheritance? Some loss-of-
462 function mutations and gene knockdowns in *C. elegans* can possibly lead to diploid maternal
463 inheritance [34,35], suggesting plausible cellular mechanisms underlying this phenomenon. During
464 normal meiosis I in *C. elegans*, the meiotic spindle migrates and orients perpendicularly to the
465 oocyte cortex. In anaphase I, one set of homologs segregates towards the cortex into the first polar
466 body while the other is retained in the oocyte. However, weak knockdown of dynein heavy chain
467 (*dhc-1*) causes the meiotic spindle to be oriented parallel to the cortex rather than perpendicular
468 during meiosis I; as a result, homologous chromosomes segregate parallel to the cortex in
469 anaphase I and no polar body is formed [35]. The half-bivalents that remain in the oocyte then
470 segregate relatively normally during anaphase II and form a polar body. The oocyte presumably

471 inherits two randomly selected homologous chromatids from each bivalent. A similar misalignment
472 of the meiotic spindle at metaphase I is also thought to be the mechanism underlying the
473 generation of diploid eggs in the obligately parthenogenetic species *Drosophila mangabeirai* [36].
474 We hypothesize that a misalignment of the meiotic spindle or a failure of cytokinesis may similarly
475 result in diploid maternal inheritance in *C. nouraguensis*.

476 What are the evolutionary consequences of this type of diploid maternal inheritance? We
477 have shown that diploid maternal inheritance in *C. nouraguensis* oocytes is the result of inheriting
478 two homologous chromatids that have undergone meiotic recombination, and therefore fits a
479 model of automixis in which two homologous chromatids are combined ("central fusion"). Because
480 there is only a single recombination event that is biased towards the chromosome ends, inheriting
481 two homologous chromatids either maintains heterozygosity across the entire chromosome or
482 most of it (Fig 3B). However, recombination does occur in the middle of chromosomes at a lower
483 frequency [26], which should eventually result in genome-wide homozygosity and inbreeding
484 depression after many generations of automixis. Most *Caenorhabditis* species are dioecious
485 (females and males), with some exhibiting genetic hyperdiversity [37,38]. Therefore, inbreeding
486 depression could be a sizable hurdle to overcome for the persistence of this form of gynogenesis
487 evolving from an obligately sexual *Caenorhabditis* ancestor.

488

489 **Females can produce males asexually**

490 Given that two copies of each maternal autosome are almost always inherited in the
491 interspecies *C. nouraguensis* x *C. becei* cross, we were surprised to observe that some diploid
492 fertile F1 are males. Indeed, sequencing data show that the three fertile males have only a single X
493 chromosome (Fig S5 and Fig S7). Thus, missegregation of the X-chromosome during the modified
494 female meiosis can result in only one X chromatid being inherited by the oocyte. Interestingly, two
495 of the three fertile males were also aneuploid (triploid) for a single *C. nouraguensis* autosome,

496 indicating that widespread chromosome missegregation occurred while producing these
497 individuals. Generating males at a low frequency can theoretically aid the spread and maintenance
498 of gynogenesis by transmitting alleles required for diploid maternal inheritance into neighboring
499 sexual populations [39]. The production of males even at a low frequency can also help propagate
500 an intraspecific gynogenetic lineage by enabling the activation of the egg and inheritance of
501 centrioles without relying on males from a related species. This is observed in the nematode
502 *Mesorhabditis belari,* in which only 9% of offspring are males and 91% are gynogenetically
503 reproducing females [30]. Thus, it is notable that the modified female meiotic segregations that
504 facilitate asexual reproduction also generate males that could promote the long-term maintenance
505 of an asexual lineage.
506

507 **Paternal genome loss**

508 In addition to diploid maternal inheritance, gynogenesis also requires paternal genome loss.
509 In viable F1 offspring from the *C. nouraguensis* x *C. becei* cross, we found that the entire haploid
510 *C. becei* paternal genome can be inherited in all cells (triploid hybrids), only a subset of cells
511 (diploid-triploid mosaic hybrids), or in no cells (fertile asexually-produced offspring) (Fig 8C). Given
512 the low frequency of viable offspring, it appears that complete loss of the paternal genome
513 (resulting in fertile offspring) or complete retention of the paternal genome (resulting in sterile
514 triploid offspring) are low frequency events. Rather, the majority of the animals likely have partial
515 losses of the paternal genome that result in aneuploidy and death of embryos.

516 Interestingly, the offspring of naturally gynogenetic fish species can have a similar spectrum
517 of paternal inheritance. Specifically, most offspring completely fail to inherit the paternal genome
518 (diploid maternal clones), but a small fraction of offspring can inherit it in a subset of cells (diploid-
519 triploid mosaic) or all cells (triploid) [29,40,41]. Given these similarities, the mechanism of paternal
520 genome loss in *C. nouraguensis* interspecies gynogenesis might be similar to that of some

521 obligately gynogenetic fish species. However, paternal genome loss can occur in a variety of
522 contexts and has different underlying causes, each of which could potentially explain the loss of
523 the *C. becei* genome [42–47]. In the context of interspecies hybridization, detailed studies in
524 *Hordeum* (barley) and *Xenopus* show that paternal chromosomes fail to recruit centromeric
525 proteins, lag during embryonic divisions, and form micronuclei [12,13]. It is noteworthy that we also
526 find lagging DNA and micronuclei in a fraction of dead *C. nouraguensis*/*C. becei* hybrid embryos,
527 potentially indicating that paternal *C. becei* chromosomes fail to load centromeric proteins required
528 for chromosome segregation.
529

530 **Asexual reproduction via hybridization**

531 In animals, fertilization by male sperm is required to reactivate the developmental program
532 of oocyte meiosis, and sperm also provide centrioles to the zygote. Thus, the evolution of
533 parthenogenetic asexual reproduction in a sexual female requires that the oocyte not rely on
534 sperm for centrioles and reactivation of meiosis. This barrier can be overcome via gynogenesis in
535 which sperm fertilize oocytes and provide meiotic reactivation and centrioles, but sperm DNA is not
536 inherited. While solving one problem, gynogenesis introduces several new problems. First, in an
537 asexual species, where do the males come from? This problem is solved in some obligately
538 gynogenetic species that are composed entirely of females and require that their eggs be fertilized
539 and activated by males of a closely related species [9]. Thus, hybridization can overcome one of
540 the major barriers to the emergence of asexual reproduction. In the hybridization studied here,
541 fertilization of *C. nouraguensis* oocytes by *C. becei* sperm leads to inheritance of paternal
542 centrioles, an altered oocyte meiosis that produces diploid eggs, and unreliable inheritance of
543 paternal DNA. Gynogenetic reproduction in this cross is rare because complete paternal genome
544 elimination is rare (Fig 8C). We hypothesize that this rare gynogenetic reproduction could serve as

545 a transitional state between sexual reproduction and more reliable interspecies gynogenetic
546 reproduction.

547 As illustrated above, a second problem for gynogenesis to overcome is the need for the
548 paternal genome to be completely and cleanly eliminated. Here again, hybridization may provide
549 part of the solution if the oocyte cytoplasm of one species does not support the reliable inheritance
550 of the paternal DNA of the other species. Such incompatibility between oocyte cytoplasm and
551 sperm DNA is far more likely between species than within species, providing another possible
552 reason that many asexual species are formed through hybridization. Hybridization may also
553 facilitate diploid maternal inheritance if incompatibilities between sperm and egg disrupt oocyte
554 meiosis and lead to the production of diploid maternal eggs, as occurs in the hybridization between
555 *C. nouraguensis* and *C. becei*. The hybrid incompatibilities observed in this cross support the
556 "balance hypothesis" that suggests how hybridization can facilitate asexual reproduction. On its
557 own, complete paternal genome elimination in the context of normal sexual reproduction would be
558 strongly deleterious as it would lead to the production of lethal haploid progeny. Likewise, diploid
559 maternal inheritance induced by sperm in the context of normal sexual reproduction would lead to
560 the production of triploid progeny that have reduced fitness (sterile in the cross we studied). But in
561 combination, these two incompatibilities can lead to the production of viable asexually-produced
562 progeny.

563 In conclusion, our study establishes the *C. nouraguensis* – *C. becei* hybridization as a new
564 genetic model system to study how hybrid incompatibilities may facilitate the emergence of rare
565 asexuality in animals. Further study of this system may provide insights into the mechanisms of
566 diploid maternal inheritance and paternal genome loss, as well as the obstacles associated with a
567 transition from sexual to asexual reproduction.

568 **MATERIALS AND METHODS**

569 ***Strain isolation and maintenance***

570 All strains of *Caenorhabditis* used in this study were derived from single gravid females
571 isolated from rotten fruit or flowers [48,49]. Strains of *C. nouraguensis* were kindly provided by
572 Marie-Anne Félix ("JU" prefix) and Christian Braendle ("NIC" prefix). Most strains are outbred,
573 except JU2079, QG2082 and QG2083, which are inbred lines derived from JU1825, QG704 and
574 QG711, respectively. These inbred lines were used to generate the *C. nouraguensis* and *C. becei*
575 genome assemblies. Strain stocks were stored at -80°. Strains were maintained at 25° on standard
576 NGM plates spread with a thin lawn of *E. coli* OP50 bacteria [50].

577

578 ***Phylogenetic analysis***

579 To construct a phylogeny, we used a subset of the coding sequences from Kiontke et al.
580 [48]. The following genes were used: *ama-1, lin-44, par-6*, *pkc-3*, *W02B12.9*, *Y45G12B.2a*,
581 *ZK686.3*, and *ZK795.3*. The *C. yunquensis* coding sequences were obtained from NCBI, while all
582 other coding sequences were obtained from the caenorhabditis.org BLAST server
583 (blast.caenorhabditis.org/#) using the *C. elegans* homolog as the query sequence. The coding
584 sequences for each species were concatenated and aligned with MUSCLE [51] using default
585 settings. A maximum likelihood phylogeny was made using PhyML 3.0 online (http://www/atgc-
586 montpellier.fr/phyml/) [52] using a Generalized Time Reversible (GTR) substitution model with six
587 substitution rate categories. Tree searching was performed using Nearest Neighbor Interchanges
588 (NNIs). Branch support was determined by 100 bootstraps.

589

590 ***Quantifying strain viability***

591 Strain viability was quantified as in [53]. Briefly, we crossed 10 virgin L4 females and males
592 of the same strain on a single plate coated with palmitic acid. The plates were placed at 25°

593 overnight, allowing the worms to mature to adulthood and begin mating. The adult worms were
594 then moved to a new plate rimmed with palmitic acid, allowed to mate and lay eggs for 1.5 hours at
595 25°, and then removed. The eggs laid within that time were immediately counted. Two days later,
596 we placed the plates at 4° for 1 hr and counted the number of healthy L4 larvae and young adults
597 per plate. We defined the percentage of viable progeny as the total number of L4 larvae and young
598 adults divided by the total number of eggs laid.
599

600 ***DIC imaging of embryogenesis***

601 Twenty-four hours after the L4 stage, we picked 20-40 gravid females into a 30 µl pool of 1x
602 Egg Buffer (25 mM HEPES pH 7.4, 118 mM NaCl, 48 mM KCl, 2 mM EDTA, 0.5 mM EGTA) on a
603 glass coverslip and dissected out embryos by cutting the adults in half using two needles like
604 scissors. The embryos were then transferred with a glass capillary tube into a fresh pool of Egg
605 Buffer to dilute any contaminating bacteria, and then placed onto a 2% agarose pad on a glass
606 slide. The mounted embryos were put into a humid chamber for 20 minutes before adding a
607 coverslip. The edges of the coverslips were sealed with petroleum jelly to prevent evaporation of
608 the agarose pad. DIC z-stack images were captured every 3 minutes for 10 hours using a Nikon
609 Eclipse 80i compound microscope (60x oil lens, 1.40 NA). Images were processed using Image J
610 [54].
611

612 ***Calculating the frequency of rare interspecific F1***

613 For each interspecies cross we set up 20-25 plates, each with one virgin L4 female crossed
614 to a single virgin L4 male. The plates were placed at 25° overnight, allowing the worms to mature
615 to adulthood and begin mating and laying eggs. To prevent overcrowding, the adult couples were
616 moved to a new plate every day for three days. The number of eggs laid on each plate was

617 counted the day the parents were removed. Each plate was monitored for two days to check for
618 the presence of rare viable F1, which were counted and moved onto a new plate.
619
620 ***Generating rare interspecific F1 and testing their fertility***
621 To collect enough rare viable F1 animals for fertility testing and genotyping, we set up six
622 cross plates, each with 30 *C. nouraguensis* L4 females and 30 *C. becei* L4 males and let them
623 develop into adults overnight at 25°. We monitored the plates for the presence of viable F1 larvae
624 each day for 5-6 days. Each viable F1 was moved to its own new palmitic acid-rimmed plate, and
625 its fertility was tested as either an L4 or young adult by backcrossing it to one or two *C.*
626 *nouraguensis* individuals of the opposite sex. F1 individuals were classified as sterile if they mated
627 to *C. nouraguensis* but produced no F2 embryos, while F1 individuals were classified as fertile if
628 they produced F2 embryos. Mating was inferred by the presence of a male-deposited copulatory
629 plug on the female vulva [55]. After fertility testing and PCR genotyping, we found that hybrid
630 males produced no embryos when crossed to *C. nouraguensis* females and were classified as
631 sterile. However, they often failed to produce a copulatory plug, so we cannot tell whether sterility
632 is due to abnormal germline development or defective mating.
633 To track the fate of the two maternal homologous chromosomes in subsequent crosses, we
634 crossed two genetically distinct strains of *C. nouraguensis* (JU1825 and NIC59) to generate
635 heterozygous *C. nouraguensis* NIC59/JU1825 females. Specifically, we crossed virgin L4 JU1825
636 females to NIC59 males and vice versa to generate female offspring that are heterozygous
637 NIC59/JU1825 at all nuclear loci and carry either JU1825 or NIC59 mitochondria, respectively. We
638 denote the genotype of these heterozygous females by the following nomenclature: “(mitochondrial
639 genotype); nuclear genotype”. Therefore, the first cross produces *C. nouraguensis* (J); N/J
640 females, while the second produces *C. nouraguensis* (N); N/J females (Table S1). We then
641 crossed both types of *C. nouraguensis* N/J virgin females to *C. becei* QG711 males. We collected

642 the rare viable F1 from these interspecies crosses and tested their fertility by backcrossing them to
643 the *C. nouraguensis* strain matching their mitochondrial genotype in order to avoid known
644 cytoplasmic-nuclear incompatibilities within this species [53].
645
646 ***Generating worm and embryo lysates for PCR***
647 Single worm PCR: Each adult worm was placed in a PCR tube with 10 µl of lysis buffer (1x
648 Phusion HF buffer + 1.0% Proteinase K) and frozen at -80° for at least 15 minutes. The worms
649 were then lysed by incubating the tubes at 60° for 60 mins and 95° for 15 mins. 1 µl of worm lysate
650 was used in each 10 µl PCR reaction. Control lysates were generated by mixing 10-15 worms in
651 lysis buffer.
652 Single embryo PCR: Dead embryos were picked into a 30 µl pool of 2 mg/ml chitinase on an
653 18x18 mm coverslip. OP50 bacteria were washed off embryos by pipetting the chitinase solution
654 up and down. Using a glass capillary tube, embryos were transferred to a new pool of chitinase
655 and washed again, and individual embryos were placed in a PCR tube with 5 µl of 2 mg/ml
656 chitinase solution and incubated at room temperature for 2 hours. 5 µl of lysis buffer (2x Phusion
657 HF Buffer + 2.0% Proteinase K) was added to each PCR tube and mixed by light vortexing. The
658 samples were then frozen and lysed as in the single worm PCR protocol. 2.5 µl of embryo lysate
659 was used in each 10 µl PCR reaction. Control lysates were generated by mixing 10-15 embryos in
660 the same PCR tube.
661
662 ***PCR primers***

Primer name	Sequence (5'-3')	Chromosome	Strains distinguished	Type of polymorphism
5.8S1	CTGCGTTACTTACCACGAATTGCAGAC	I (ITS2)	*C. n* vs *C. b*	PCR-RFLP (Hind-III)

KK-28S-22	CACTTTCAAGCAACCCGAC	I (ITS2)	*C. n* vs *C. b*	PCR-RFLP (Hind-III)
oPL20	CTGATGAGCATCGTCCGAC	II (W02B12.9)	*C. n* vs *C. b*	PCR-RFLP (EcoRI)
oPL21	CCTAGCTTGCAATCCACACG	II (W02B12.9)	*C. n* vs *C. b*	PCR-RFLP (EcoRI)
oPL78	TCCTCCAGCATATCCGCTCG	III	JU1825 vs NIC59	indel
oPL79	CAATTGCACGGAGAGACTGTTCATC	III	JU1825 vs NIC59	indel
oPL181	CGTCAAGATCAGATGCGAGACG	I	JU1825 vs NIC59	indel
oPL182	CAGTTGAGAACTGCCTGTCAGAC	I	JU1825 vs NIC59	indel
oPL318	GTGGCTTGTAGAGCTTGTGC	V	*C. n* vs *C. b*	indel
oPL319	GATCAATGATAGACATGGCC	V	*C. n* vs *C. b*	indel
oPL320	TGGTGTCGAATTCTCAAATTCC	X	*C. n* vs *C. b*	indel
oPL321	TAGGGGCAGAATATTGAACACTG	X	*C. n* vs *C. b*	indel
oPL356	TATTTGTGTGTTTGCCAGAGG	V	JU1825 vs NIC59	indel
oPL357	TCGAATACATTTGGCTTCACG	V	JU1825 vs NIC59	indel

663

664 The primers used in the PCR-RFLP polymorphism assays lie in conserved coding

665 sequences that are easily amplified from a range of *Caenorhabditis* species [48]. Primers 5.8S1

666 and KK-28S-22 were originally used in Kiontke et al [48]. The primers used in the PCR indel
667 polymorphism assays were generated after the assembly of the *C. nouraguensis* genome. Indel
668 polymorphisms between NIC59 and JU1825 were found by manually screening *C. nouraguensis*
669 (JU2079) scaffolds in IGV [56] for regions where JU1825 had read coverage but NIC59 did not
670 (and vice versa). Indel polymorphisms between *C. nouraguensis* and *C. becei* were manually
671 found by aligning homologous sequences on scaffolds assigned to a chromosome of interest.
672

673 ***Fixing and DAPI staining the female germline***

674 Fixing and DAPI staining germlines was performed as in [57]. F1 L4 females were mated to
675 *C. nouraguensis* L4 males. 24 hours later, we dissected the gonads from fertile F1 females and
676 stained with DAPI. 30-40 females were picked into 15 µl of 1x Egg Buffer + 0.1% Tween-20 on a
677 glass coverslip and their heads were cut off with needles to expel the gonad. After dissection, 15 µl
678 of Fixation Solution (1x Egg Buffer + 7.4% formaldehyde) was added and mixed well by pipetting.
679 Gonads were fixed for 5 minutes, then 15 µl of the mixture was removed and a Histobond slide
680 was laid down gently on top of the coverslip. Excess liquid was removed with Whatman paper and
681 samples were frozen by placing the slide on a metal block on dry ice for 10 minutes. Coverslips
682 were then quickly flipped off with a razor blade and the slides were placed in a Coplin jar with -20°
683 methanol for 1 minute. The slides were then moved to a Coplin jar with 1x PBS + 0.1% Tween-20
684 for 10 minutes, then a Coplin jar with 1x PBS + 0.1% Tween-20 + 5 µl of 5 mg/ml DAPI for 15
685 minutes, then a Coplin jar with 1x PBS + 0.1% Tween-20 for 20 minutes. Samples were then
686 mounted with 11 µl Mounting Media (35 µl 2M Tris + 15 µl MilliQ dH_2O + 450 µl glycerol) and
687 sealed with nail polish. Images were taken using a Nikon Eclipse 80i compound microscope and
688 processed using Image J.
689

690 ***C. becei genome assembly and linkage map construction***

691 The chromosomal reference assembly for *C. becei* is based on high-coverage paired-end
692 and mate-pair short-read sequencing, low-coverage Pacific Biosciences long reads, and genetic
693 linkage information from an experimental intercross family. We used two inbred lines, QG2082 and
694 QG2083, derived from isofemale lines QG704 and QG711 respectively by sib-mating for 25
695 generations. QG704 and QG711 were isolated from independent samples of rotten flowers
696 (QG704) or fruit (QG711) collected in Barro Colorado Island, Panama, in 2012 [49]. We generated
697 conservative *de novo* assemblies for the inbred lines, identified SNPs that distinguish them, and
698 then used a six-generation breeding design to generate recombinant populations (G_4BC_2) from
699 which we generated a SNP-based linkage map. With the map-scaffolded conservative assembly,
700 we were able to evaluate more contiguous, less conservative genome assemblies for consistency,
701 and we selected one of these as our final *C. becei* genome. Each of these steps is described in
702 detail below.
703
704 *Sequencing*
705 We extracted genomic DNA from QG2083 by proteinase K digestion and isopropanol
706 precipitation [58] and prepared paired-end (PE) 600-bp insert and mate-pair (MP) 4-kb insert
707 Illumina Nextera libraries, from which 100-bp reads were sequenced to approximately 30x and 60x
708 expected coverage (see below) on an Illumina HiSeq 2000 at the NYU Center for Genomics and
709 Systems Biology GenCore facility (New York, USA). PE reads for QG2082 were generated
710 similarly, for 20x expected coverage. PE reads for G_4BC_2 mapping populations were generated
711 from 250bp insert libraries sequenced to mean 4x coverage per line with 150-bp reads on a HiSeq
712 2500. FASTX Toolkit (v. 0.0.13; options '-n -l 25 -M 9 -Q 33';
713 http://hannonlab.cshl.edu/fastx_toolkit/) was used to trim low quality bases from PE reads, and
714 NextClip (v. 1.3; [59]) was used to remove adaptors from MP reads and assess read orientation.
715 Contaminating bacterial sequence was removed with Kraken (v. 1.0; [60]) using a database built

716 from NCBI nt (downloaded 10/06/2014), and sequencing errors were corrected with Blue (v. 1.1.2;
717 [61]). Raw data is available from the NCBI SRA under project PRJNA525787.
718
719 *Genome assembly for map construction*
720 We assembled contigs and conservative scaffolds for QG2083 with the string graph
721 assembler SGA [62]. Scaffolding required contigs to be linked by at least 5 unambiguously
722 mapped mate-pair reads and full path consistency between contigs and all mapped mate-pair
723 reads (option '--strict'). PacBio long reads (12x coverage, P4-C2 chemistry, Duke University Center
724 for Genomic and Computational Biology) were used for a single round of gap closing and
725 scaffolding with PBJelly (v. 13.10, minimum evidence of two reads; [63]), followed by scaffold
726 breakage at any regions of mate-pair read discordance with REAPR (v. 1.0.17; [64]). This yielded
727 a fragmented assembly of 9152 scaffolds of length at least 500 bp spanning 95.9 Mb, with half the
728 assembly in scaffolds of 56 kb or more.
729
730 *Variant calling*
731 QG2082 reads were aligned to the QG2083 reference scaffolds with bwa mem (v. 0.5.9;
732 [65]), processed with samtools (v. 1.2; http://www.htslib.org/) and Picard (v. 1.111;
733 http://broadinstitute.github.io/picard/) utilities, and SNPs were called using the GATK
734 HaplotypeCaller (v. 3.1-1; hard filtering on 'MQ < 40.0 || DP < 4 || FS > 60.0 || ReadPosRankSum <
735 -8.0 || QD < 4.0 || DP > 80'; [66]). Fixed diallelic SNPs were supplemented with calls from
736 reference mapping of the pooled G_4BC_2 data and, to mitigate potential mapping bias against highly
737 divergent regions, SNP calls from whole genome alignment of a *de novo* assembly of G_4BC_2 data
738 pooled with QG2083 data at 1:1 expected heterozygosity, using the heterozygous aware
739 assembler Platanus [67] and Mummer [68]. This yielded a total of 1.63M diallelic SNPs across
740 6843 scaffolds spanning 89.2 Mb. These SNPs provide markers for genetic map construction.

741

742 *Genetic map construction*

743 We generated F_2 animals from reciprocal crosses between QG2083 and QG2082. We then
744 performed 160 single-pair random-mating intercrosses among F_2s to generate G_3s, and again
745 among G_3s to generate G_4s. These intercrosses allow additional meioses to expand the genetic
746 map. We backcrossed G_4 females to QG2082 males, generating progeny carrying one
747 recombinant version of the genome and one intact QG2082 genome. To increase the quantity of
748 DNA representing these genomes, we crossed females to QG2082 males again and allowed the
749 resulting G_4BC_2 populations to grow for a single generation before DNA extraction and library
750 preparation. Data for 87 G_4BC_2 populations with at least 0.5x expected coverage were mapped to
751 the QG2083 scaffolds and genotyped by HMM using a modified MSG pipeline (assuming six
752 crossovers per assembled genome, genotyping error rates of 0.001, and a scaling parameter on
753 transition probabilities of $1x10^{-11}$, taking the dominant parental assignment as a single genotype for
754 each scaffold) [69]. Markers were filtered in r/qtl based on missing data (<50%) and segregation
755 distortion (χ^2 test $p > 1x10^{-10}$), followed by removal of redundant markers [70]. Based on
756 genotyping error rate estimates we further required a minimum of 70 SNP calls per scaffold and a
757 minimum length of 1 kb, yielding 1337 non-redundant scaffold markers spanning 81.5 Mb. Six
758 linkage groups were recovered over a wide range of minimum pairwise LOD scores, and within
759 linkage group marker ordering was carried out by the minimum spanning tree method implemented
760 in ASMap [71].

761

762 *Assembly of the C. becei draft genome*

763 Linkage group scaffolds were aligned against multiple Platanus *de novo* assemblies using
764 the sequencing data from inbred lines and subsampling of the approximately 350x pooled data
765 from G_4BC_2 lines, with the UCSC chain/net pipeline [72]. Genome evolution in the *Caenorhabditis*

766 genus occurs largely through intrachromosomal rearrangement, and 84-94% of the net for each *C.*
767 *becei* linkage group aligned to the homologous *C. elegans* chromosome. The assembly most
768 concordant with genetic data was selected, based on the number and aligned length of (1)
769 scaffolds mapping to multiple linkage groups and (2) outliers in the ratio of genetic to physical
770 distance. The selected assembly contained six cases where scaffolds mapped to multiple linkage
771 groups – usually terminal regions of large scaffolds, with these terminal alignments spanning just
772 over 1 Mb in total – and three scaffolds where mapping within linkage groups was inconsistent with
773 the genetic data (median absolute deviation 99th percentile for the ratio of genetic to physical
774 span), spanning 179 kb.

775 The draft assembly improved contiguity and incorporated several Mb of sequence not
776 represented by the genetic map scaffolds, from 2483 redundant marker scaffolds to 256 final
777 scaffolds spanning 84.9 Mb. We estimate a genome size of around 95 Mb based on mapped read-
778 depth [62], with 90 Mb of that unique sequence amenable to assembly and variant calling.

779

780 ***C. nouraguensis genome assembly***

781 The *C. nouraguensis* reference genome was generated from JU2079, an inbred strain
782 derived from 28 generations of JU1825 sibling matings (Marie-Anne Félix, personal
783 communication). Genomic DNA and RNA were purified from mixed-stage individuals and sent to
784 Mark Blaxter at the University of Edinburgh for Illumina sequencing. 125-bp paired-end reads were
785 generated from two libraries, one with inserts of ~400 bp (~55 million read-pairs), the other with
786 inserts of ~550 bp (~54 million read-pairs) (SRA project accession PRJEB10884). After generating
787 a preliminary assembly, we used BlobTools [73] for taxonomic classification. Some contigs
788 matched *E. coli* (provided as food) and some matched an unsequenced bacterial species in the
789 Firmicutes phylum. We extracted the Firmicutes contigs and used GSNAP [74] to remove matching
790 read-pairs, and to remove any read-pairs matching the *E. coli* REL606 genome (Genbank

791 accession NC_012967), a strain closely related to OP50. We also removed reads failing Illumina's
792 'chastity filter' and used cutadapt to trim poor quality sequences (phred score < 10) and adapter
793 sequences from the 3' ends of reads. We then performed error-correction using Musket [75] with a
794 k-mer size of 28, and performed *de novo* genome assembly, scaffolding and gap closure using
795 Platanus [67] with an initial k-mer size of 21. We then used REAPR [64] to break any
796 misassembled scaffolds. The resulting assembly is approximately 73 Mb in size. We used BUSCO
797 [76] to measure its completeness using a set of conserved genes, and find that our assembly
798 contains 81.5% of conserved single-copy orthologs as a single copy, 9.8% as duplicates, and 3.6%
799 as fragments, very similar to what is seen in the finished *C. elegans* genome assembly [76]. Using
800 MUMMER [68], we ordered and oriented our *C. nouraguensis* scaffolds based on synteny to the *C.*
801 *becei* genome assembly. Using this approach, some scaffolds remain unplaced and others may be
802 misplaced, either because of true differences between the two species' genomes, or because
803 MUMMER's alignments are noisy.
804 We also generated assemblies of the mitochondrial genomes of *C. becei* strain QG2083,
805 and *C. nouraguensis* strain JU2079 using reads generated by Mark Blaxter's lab (EMBL ENA
806 accession ERR1018617), filtered as above to remove *E. coli* reads, and down-sampled to 10
807 million read-pairs for *C. nouraguensis*. We then used the Assembly by Reduced Complexity (ARC)
808 [77] pipeline to assemble mitochondrial genomes, using the *C. elegans* mitochondrial genome
809 sequence as a starting point.
810
811 ***Whole-genome amplification and library preparation***
812 After testing the fertility of rare viable offspring from crosses of *C. nouraguensis*
813 JU1825/NIC59 females to *C. becei* males (see above), we prepared Illumina whole-genome
814 sequencing libraries as follows. We first transferred each worm individually to a blank NGM plate
815 with no OP50 lawn for 30 minutes to reduce the amount of contaminating bacterial DNA. We then

816 performed whole-genome amplification using the Qiagen REPLI-g Single Cell kit [78]. We picked
817 individual worms into 4 µl of PBS sc and froze them at -20° for at least an hour. We thawed the
818 samples and added 3 µl of Buffer D2, mixed well, and incubated at 65° for 20 minutes rather than
819 the recommended 10 minutes to aid in worm lysis. The rest of the protocol was performed
820 according to the manufacturer's guidelines. We purified the resulting amplified DNA using the
821 Zymo Research Genomic DNA Clean & Concentrator kit (gDDC-10). We submitted approximately
822 0.5-0.8 ng of each sample to the Fred Hutchinson Cancer Research Center Genomics Core
823 Facility. A uniquely barcoded sequencing library for each sample was made using the Illumina
824 Nextera library prep kit and sequenced on an Illumina Hiseq2500 to generate 50-bp paired-end
825 reads. We sequenced eleven fertile and ten sterile F1 individuals. We also sequenced a set of
826 control samples so that we could determine how coverage varies across the genome for pure *C.*
827 *nouraguensis* or *C. becei* populations, as well as to allow us to determine fixed SNPs between the
828 NIC59 and JU1825 *C. nouraguensis* strains. Specifically, we sequenced genomic DNA derived
829 from large populations of NIC59, JU1825 and QG711 (sample names: NIC59_bulk, JU1825_bulk
830 and QG711_bulk). In order to determine whether SNP frequencies and coverage metrics behave
831 as expected in heterozygous or hybrid triploid genomes, we sequenced three additional controls:
832 (a) a single heterozygous NIC59/JU1825 female (sample name: F1_NIC59_JU1825); (b) a sample
833 where we placed one NIC59 female and one JU1825 female in the same tube (sample name:
834 NIC59plusJU1825); and (c) a sample where we placed one NIC59 female, one JU1825 female and
835 one QG711 female in the same tube (sample name: NIC59plusJU1825plusQG711).
836

837 ***SNP calling, genotyping, and coverage calculations***

838 Using GSNAP [74], we mapped the reads from each sample to a combined reference
839 genome containing the *C. nouraguensis* and *C. becei* nuclear and mitochondrial genome
840 assemblies, the *E. coli* REL606 genome sequence and the Firmicutes contigs described above.

841 We allowed GSNAP to report only a single map position for each read (--npaths=1). We further
842 filtered read mappings, requiring mapq value of at least 20 to select uniquely mapping reads.
843 After preprocessing bam files by marking duplicates (using picard's MarkDuplicates,
844 http://broadinstitute.github.io/picard/) and realigning indels (using GATK's RealignerTargetCreator
845 and IndelRealigner tools [66]), we called SNPs in *C. nouraguensis* scaffolds using samtools
846 mpileup [79] (ignoring indels, disabling the per-base alignment quality option and increasing the
847 depth down-sampling parameter to 6660). We counted reads matching each allele using GATK's
848 VariantAnnotator tool [66], disabling the down-sampling option and using the
849 "ALLOW_N_CIGAR_READS" option. We noticed that the distribution of allele frequencies in our
850 'heterozygous' control samples was skewed towards the reference allele, likely because those
851 reads are easier to map to the reference assembly. We therefore used this first round of SNP calls
852 to remap all reads to the combined reference genome using GSNAPs "SNP-tolerant" mode that
853 allows reads to map to either haplotype. SNPs were called a second time, after one additional level
854 of read mapping filtering, where we used the R/Bioconductor Rsamtools package [80] to select
855 only reads where the full length of the read could be aligned to the reference genome.
856 We then used the R/Bioconductor VariantAnnotation package [80] to select high-quality
857 fixed differences between the NIC59 and JU1825 strains as follows: we required a SNP quality
858 score of at least 100; that opposite alleles be fixed (non-reference frequencies of <5% and >95%)
859 in the two strains; that read depth in some *C. nouraguensis* control samples be within typical range
860 for that sample (5-50 for JU1825_bulk and NIC59_bulk, and 100-450 for the combined JU2079
861 samples); and that read depth be 0 in our *C. becei* control samples (QG711_bulk and the two
862 QG2083 libraries). 337,493 SNPs passed these filters (an average of one SNP every 217 bp). To
863 estimate mean allele frequencies in 50-kb windows across the genome, we counted the total
864 number of reads matching NIC59 and JU1825 alleles across the window and divided the NIC59
865 count by the total count. We then used a circular binary segmentation algorithm, implemented in

866 the Bioconductor package DNAcopy [81], to estimate the locations of breaks between different
867 haplotypes as well as the average allele frequency in each segment.
868 Using the same filtered bam files, we determined coverage at each base position using the
869 samtools depth tool [79]. Examining coverage and aligned bases in our control samples
870 (JU1825_bulk, NIC59_bulk and QG711_bulk) reveals very high within-species sequence diversity,
871 as seen in some other nematodes [37,38,82]. This high diversity means that in some genomic
872 regions, especially on the chromosome arms, short reads are unalignable to the reference
873 genomes, resulting in many regions of no coverage. Other genomic regions show more aligned
874 base-pairs, but still harbor many SNPs. Therefore, before calculating mean coverage metrics, we
875 filtered the base positions under consideration to include only those that had coverage of at least 8
876 reads in the relevant control samples (JU1825_bulk and NIC59_bulk for the *C. nouraguensis*
877 assembly and QG711_bulk for the *C. becei* assembly), and then determined mean values in 50-kb
878 regions of each scaffold. This filtering mitigated diversity-related coverage variation a little, but
879 even in control samples coverage is still lower on chromosome arms than centers. To generate
880 per-chromosome copy number estimates (Fig. 4A), we manually defined 1-2 regions in the center
881 of each chromosome that are well-covered in each of the control samples and took the mean of
882 50-kb window coverages in each region.
883
884 ***Fixing and staining embryos***
885 60-80 gravid females were picked into 30 µl of 1x Egg Buffer + 0.1% Tween-20 on a glass
886 coverslip and dissected in half with needles to release embryos. After the females were dissected,
887 we waited for five minutes to allow the mostly 1-cell stage embryos to develop. A Histobond slide
888 was then gently laid on top of the coverslip. Excess liquid was removed with Whatman paper and
889 the samples were frozen by placing the slide on a metal block on dry ice for 10 minutes. Coverslips
890 were then quickly flipped off with a razor blade and the slides were immediately placed in a Coplin

891 jar with -20° methanol for 10 min. The slides were then moved to a Coplin jar with -20° acetone for
892 10 min. The slides were washed three times for 10 mins each in Coplin jars with 1x PBS + 0.1%
893 Tween-20, then blocked for 30 mins in a Coplin jar with 1x PBS + 0.1% Tween-20 + 0.5% BSA +
894 0.02% sodium azide (blocking buffer). Each slide was then incubated overnight at 4° with a 1:100
895 dilution of both mouse monoclonal anti-α-tubulin (clone DM1A, Sigma) and rabbit polyclonal anti-γ-
896 tubulin (ab50721, abcam) primary antibodies in blocking buffer. The next day, the slides were
897 washed three times for 10 mins each in Coplin jars with 1x PBS + 0.1% Tween-20. Each slide was
898 then incubated in the dark for 2 hours at room temperature with a 1:1000 dilution of both Alexa-
899 Fluor 488 goat anti-mouse and Rhodamine Affinipure goat anti-rabbit secondary antibodies
900 (Jackson ImmunoResearch) diluted in 1x PBS + 0.1% Tween-20. The slides were moved to a
901 Coplin jar with 1x PBS + 0.1% Tween-20 for 10 minutes, then a Coplin jar with 1x PBS + 0.1%
902 Tween-20 + 5 µl of 5 mg/ml DAPI for 15 minutes, then a Coplin jar with 1x PBS + 0.1% Tween-20
903 for 20 minutes. Samples were mounted with 12 µl VectaShield (H-1000, Vector Laboratories) and
904 sealed with nail polish. Samples were imaged using a Nikon Eclipse 80i compound microscope
905 with a 100x oil objective (1.45 NA). Images were processed using Image J.
906 We only analyzed embryos at early stages of embryogenesis (1-4 cell stage). In normal
907 embryos at this stage, the DNA in the two polar bodies appears as two distinct clumps at the
908 periphery of the embryo that are easily distinguishable from other embryonic nuclei. Polar bodies in
909 hybrid embryos were considered to have abnormal morphologies if they were unlike those
910 observed in the JU1825 control. This encompasses a range of abnormalities such as not being
911 round, being larger, or having easily distinguishable chromatids.
912
913 ***Male UV irradiation***
914 Virgin *C. nouraguensis* L4 males and L4 females were collected and separately placed onto
915 two new NGM plates seeded with OP50 and rimmed with palmitic acid. We added a few females to

916 the male plate to coax the males to stay on the surface of the plate. The next day, now young adult
917 males were picked onto a blank NGM plate rimmed with palmitic acid. This plate was placed in a
918 CL-1000 UV Crosslinker (Ultra-Violet Products) without a lid and the males were exposed to
919 70,000 μJ/cm^2 254-nm UV radiation. Immediately afterward, the males were picked onto new NGM
920 plates seeded with OP50 and rimmed with palmitic acid. Each plate had 30-90 irradiated males
921 and 30-90 young adult virgin females. The next day, rare viable larvae were picked from the cross
922 plates onto a new NGM plate seeded with OP50 and rimmed with palmitic acid. When these
923 progeny reached adulthood, they were individually frozen, lysed and PCR genotyped.

924 We tested the following UV exposures: 15,000, 40,000, 50,000, 60,000, 70,000, 80,000,
925 150,000 and 250,000 μJ/cm^2. Males treated with lower exposures (15,000 and 40,000 μJ/cm^2)
926 were able to produce many viable progeny, indicating that their sperm DNA was not damaged
927 enough to induce paternal genome loss. Males treated with the highest exposures (150,000 and
928 250,000 μJ/cm^2) mostly stopped moving and never recovered. We found that males treated with
929 70,000 μJ/cm^2 were healthy enough to mate and produce many dead fertilized embryos, but
930 relatively few viable progeny.

931 Each 30 female x 30 male or 90 female x 90 male plate eventually became overcrowded
932 with dead embryos, making it difficult to manually quantify their exact number. Instead of counting
933 each embryo on these plates, we performed a five female x five male cross in parallel and counted
934 their dead embryos. We then determined the average number of dead embryos per female on the
935 5 female x 5 male plates and multiplied that by the number of total females to get a rough estimate
936 of the total number of dead embryos.

937

938 **ACKNOWLEDGMENTS**

939 We thank Marie-Anne Félix and Christian Braendle for providing the strains of *C.*
940 *nouraguensis* used in this study; Max Bernstein, Vicky Cattani, Taniya Kaur, Jasmine Nicodemus

941 and Annalise Paaby for help performing *C. becei* mapping crosses and preparing sequencing
942 libraries; Mark Blaxter, Lewis Stevens and members of the *Caenorhabditis* Genomes Project for
943 sequencing *C. nouraguensis* (JU2079) as well as providing a public BLAST server of newly
944 sequenced *Caenorhabditis* species (http://blast.caenorhabditis.org/); Maulik Patel for help in
945 preparing DNA for *C. nouraguensis* genome sequencing (JU1825 and NIC59); Lews Caro and
946 Sam Hart for additional experiments; Jihong Bai for sharing his UV-irradiator; Lamia Wahba for
947 advice on single-worm sequencing; Needhi Bhalla and Mara Schvarzstein for discussions of *C.*
948 *elegans* female meiosis; Jim Priess for discussions of *C. elegans* development; and Hannah Seidel
949 for advice on time-lapse imaging of *Caenorhabditis* embryos. We also thank Barbara Wakimoto,
950 Diane Shakes, Lisa Kursel, Irini Topalidou, Ofer Rog and members of his lab, and members of the
951 Ailion lab for comments on the manuscript. We thank the Fred Hutchinson Genomics core for
952 Illumina library preparation and sequencing.

953

954 **FIGURE CAPTIONS**

955 **Fig 1. Crossing *C. nouraguensis* females to *C. becei* males results in sterile F1 with hybrid**
956 **genotypes and fertile F1 with only-maternal genotypes. (A)** A maximum likelihood phylogeny of
957 several *Caenorhabditis* species closely related to *C. nouraguensis* and *C. becei*, with strain names
958 in parentheses. *C. elegans and C. remanei* were used as outgroups. The scale bar represents
959 0.10 substitutions per site. Bootstrap support values are indicated to the left of each node (percent
960 of 100 bootstrap replicates). See Stevens et al. (2019) for a more complete *Caenorhabditis*
961 phylogeny [49]. **(B)** Frequency of viable F1 adults in crosses between *C. nouraguensis* and *C.*
962 *becei*. NIC54 females yield a significantly higher proportion of viable F1 adults when crossed to *C.*
963 *becei* (QG711) males than either JU1825 or NIC59 females (Chi-square with Yates correction,
964 P=0.0065 NIC54 vs. JU1825, P=0.0005 NIC54 vs. NIC59). There was not a significant difference
965 in the frequency of rare viable F1 adults produced by JU1825 and NIC59 females (Chi-square with

966 Yates correction, P=0.49). The crosses between *C. becei* females and *C. nouraguensis* males
967 serve as controls for accidental contamination of plates with embryos or larvae from either parental
968 species -- no viable adults were found among more than 12,000 F1 screened for each cross (Fig
969 S2). **(C)** Flowchart showing how fertility of rare viable F1 was tested (also see Materials and
970 Methods). The gel shows how a PCR-RFLP assay distinguishes between *C. nouraguensis* and *C.*
971 *becei* alleles at the ITS2 locus. **(D)** Tables showing the relationship between the fertility, genotype,
972 and sex of rare viable F1 derived from crossing either *C. nouraguensis* (JU1825) females to *C.*
973 *becei* (QG711) males (top table, genotyped at the W02B12.9 locus) or *C. nouraguensis* (NIC54)
974 females to *C. becei* (QG711) males (bottom table, genotyped at the ITS2 locus). Both sterile and
975 fertile F1 exhibited a more strongly female-biased sex ratio than that seen in intraspecies crosses
976 (Fig S1A).
977
978 **Fig 2. Asexually-produced F1 females are diploid**. **(A)** Schematic of one of the two germlines of
979 a *Caenorhabditis* female. The germline is a syncytial tube with nuclei (depicted as small circles)
980 hugging its circumference. Germline nuclei are generated from mitotically dividing stem cells at the
981 distal tip and migrate proximally while undergoing meiotic prophase. Homologs of each of the six
982 chromosomes replicate their DNA, with the resulting sister chromatids held together by sister
983 chromatid cohesion (purple lines). Homologous chromosomes undergo one crossover biased
984 towards a chromosome end and are remodeled into a cruciform structure. Eventually, cell
985 membranes form around the nuclei, resulting in mature oocytes. In mature oocytes, homologous
986 chromosomes and their sister chromatids form bivalents that are held together by a combination of
987 sister chromatid cohesion and recombination. The -1 oocyte is fertilized by sperm, triggering the
988 reductional first meiotic division in which sister chromatid cohesion is lost between homologs,
989 allowing them to segregate during anaphase I. One set of homologs is segregated into the first
990 polar body. During the second meiotic division, sister chromatid cohesion is lost between sister

991 chromatids, which then segregate during anaphase II. One chromatid is segregated into the
992 second polar body and the other is inherited by the oocyte. **(B)** Because only one crossover occurs
993 per homologous set of chromosomes, diploid individuals have six bivalents (6 DAPI-staining
994 bodies) while triploids have six bivalents and six univalents (12 DAPI-staining bodies). **(C)** Most *C.*
995 *nouraguensis* (JU1825), *C. becei* (QG711) and fertile F1 females have 6 DAPI-staining bodies,
996 consistent with being diploid for six chromosomes. However, some fertile F1 females have a
997 slightly higher number of DAPI-staining bodies, suggesting they are mostly diploid, but inherit
998 some extra pieces of DNA. See Fig S4 for examples of DAPI staining.
999

1000 **Fig 3. Asexually-produced fertile interspecific F1 inherit two randomly selected homologous**
1001 **chromatids from each maternal bivalent. (A)** Schematic of how we determined which two
1002 chromatids are inherited from each maternal *C. nouraguensis* bivalent. Two genetically distinct
1003 strains of *C. nouraguensis*, NIC59 and JU1825, were crossed to make heterozygous
1004 NIC59/JU1825 females, which were then crossed to *C. becei* (QG711) males. Viable F1 progeny
1005 were collected, assayed for fertility by backcrossing, and prepared for whole-genome amplification
1006 and sequencing. **(B)** The six possible ways to inherit two chromatids from a bivalent. Four have
1007 distinct chromosomal genotypes (Sisters_1, Sisters_2, Homologs_1 and Homologs_2), and two
1008 have genotypes that cannot be distinguished in our short-read sequencing data because they both
1009 result in heterozygosity across the entire chromosome (Homologs_3). **(C)** An example of whole-
1010 genome genotyping data from a single fertile F1 female (F1_5). Each plot represents one of the six
1011 chromosomes. Each point represents the average NIC59 SNP frequency in 50-kb windows
1012 ordered along the chromosome; haplotype change points and average allele frequency for each
1013 segment are shown by the green horizontal lines. The reference assembly is fragmented into
1014 scaffolds that we ordered and oriented on chromosomes using synteny; gray vertical lines
1015 represent breaks between scaffolds. The combination of two chromatids that best matches the

1016 genotyping data is shown underneath each plot. Genotyping and coverage plots for all F1 are
1017 shown in Figs S5 and S7. One fertile F1 gave ambiguous genotypes and was excluded from
1018 further analysis (F1_25); this individual had a particularly high percentage of contaminating
1019 bacterial reads and low coverage of the *C. nouraguensis* genome (Table S1). **(D)** Frequency of the
1020 five distinguishable chromosome genotypes when combining all fertile F1 genotyping data. The
1021 table also shows the expected frequency of the five genotypes if any two chromatids were
1022 randomly inherited and if any two homologous chromatids were inherited. The frequencies
1023 observed in the fertile F1 are not different from those expected from random inheritance of two
1024 homologous chromatids (Fisher's exact test, P=0.41). Hemizygous X chromosomes in males and
1025 triploid autosomes were excluded from the analysis.
1026
1027 **Fig 4. Sterile interspecific F1 inherit a diploid *C. nouraguensis* genome and a haploid *C.*
1028 *becei* genome. (A)** The normalized read coverage for all autosomes in eight sterile F1 with a clear
1029 genotype. Coverage is normalized to the *C. nouraguensis* chromosome I coverage in each
1030 individual, which is set to two. Schematics below the graph show sterile F1 that are fully triploid
1031 hybrids (all cells of an F1 embryo have a diploid *C. nouraguensis* genome and a haploid *C. becei*
1032 genome) or diploid-triploid mosaic hybrids (all cells of an F1 embryo have a diploid *C.*
1033 *nouraguensis* genome, but only a subset of cells inherit the haploid *C. becei* genome). **(B)** An
1034 example of whole-genome *C. nouraguensis* genotyping data from a single sterile F1 male (F1_17).
1035 Each plot represents one of the six chromosomes. Each point represents the average NIC59 SNP
1036 frequency (after removing *C. becei* reads) in 50-kb windows along the physical length of the
1037 chromosome; haplotype change points and average allele frequency for each segment are shown
1038 by the green horizontal lines. The gray vertical lines represent breaks between scaffolds. The
1039 combination of two *C. nouraguensis* chromatids that best matches the genotyping data is shown
1040 underneath each plot. Genotyping and plots for all sterile F1 are shown in Figs S5 and S7. We

1041 excluded two sterile F1 from further analysis because they gave ambiguous genotypes (F1_18 and
1042 F1_26). **(C)** Frequency of the five distinguishable *C. nouraguensis* chromosome genotypes when
1043 combining all sterile F1 genotyping data. The table also shows the expected frequency of the five
1044 genotypes if any two chromatids were randomly inherited and if any two homologous chromatids
1045 were inherited. The frequencies observed in the sterile F1 are not different from those expected
1046 from random inheritance of two homologous chromatids (Fisher's exact test, P=0.78). **(D)**
1047 Frequency of *C. nouraguensis* chromosome genotypes when combining all fertile and sterile F1
1048 genotyping data. The frequencies observed are not different from those expected from random
1049 inheritance of two homologous chromatids (Fisher's exact test, P=0.85).
1050
1051 **Fig 5. Dead interspecific F1 embryos inherit the *C. becei* X-chromosome and two maternal**
1052 **homologous chromatids. (A)** Schematic illustrating how dead F1 embryos and viable F1 progeny
1053 were generated for PCR genotyping experiments. **(B)** An example of a DNA gel showing the
1054 chromosome X genotypes (oPL320+321) of rare viable F1 adults (top gel) and dead F1 embryos
1055 (bottom gel). The graph shows that no viable F1 animals inherited the *C. becei* X-chromosome, but
1056 half of the dead embryos inherited it. **(C)** An example of a DNA gel showing the chromosome V
1057 genotypes (oPL318+319) of dead F1 embryos. The graph shows that most dead F1 embryos
1058 inherited chromosome V from both parents but that some inherited only a maternal (*C.*
1059 *nouraguensis*) copy. **(D)** An example of a DNA gel showing the chromosome I genotypes
1060 (oPL181+182) of dead F1 embryos. Importantly, the primers used in this PCR reaction do not
1061 produce products when using a control *C. becei* QG711 embryo lysate as template, so any signal
1062 should be from *C. nouraguensis* templates. The graph shows that almost all dead F1 embryos
1063 have a heterozygous NIC59/JU1825 genotype. **(E)** A one-cell stage embryo derived from crossing
1064 *C. nouraguensis* (NIC59) females to *C. nouraguensis* (NIC59) males, fixed and stained for DNA
1065 (cyan), γ-tubulin (magenta), and α-tubulin (yellow). γ and α-tubulin staining shows the mitotic

1066 spindle, which helps determine how many cells there are in the embryo and at what point those
1067 cells are in the cell cycle. The white lines outline cells. The two polar bodies that remain associated
1068 with the embryo are indicated by arrowheads. **(F)** An intraspecies *C. nouraguensis* embryo with
1069 only one polar body. **(G)** A hybrid embryo with only one polar body, derived from crossing *C.*
1070 *nouraguensis* (NIC59) females to *C. becei* (QG711) males. **(H)** A hybrid embryo with zero polar
1071 bodies. Scale bars (E-H): 20 μm. **(I)** Roughly half the hybrid embryos have only one polar body. By
1072 contrast, embryos derived from *C. nouraguensis* intraspecies crosses almost always have two
1073 polar bodies. "Two abnormal" refers to embryos that have two polar bodies, but one or both have
1074 an abnormal structure. "One abnormal" refers to embryos that have a single polar body with an
1075 abnormal structure.
1076
1077 **Fig 6. Cytological characterization of early embryonic development in interspecies hybrids.**
1078 **(A-H)** A set of fixed embryos that summarize early embryonic development in *C. nouraguensis*
1079 intraspecies crosses (NIC59 female x NIC59 male). Embryos stained for DNA (cyan), α-tubulin
1080 (yellow) and γ-tubulin (magenta). Scale bars: 20 μm. **(A)** When the sperm fertilizes the oocyte, it
1081 deposits a condensed haploid paternal genome ("p") and centrioles into the egg. The centrioles
1082 gather γ-tubulin, which nucleates microtubule polymerization (two magenta dots). Fertilization
1083 triggers the female meiotic divisions, resulting in two polar bodies ("pb") and the formation of a
1084 haploid maternal pronucleus ("m"). **(B)** The two pronuclei decondense and migrate towards each
1085 other. Centrosomes remain associated with the paternal pronucleus. **(C)** The two pronuclei meet.
1086 **(D)** Maternal and paternal chromosomes align along the metaphase plate of the first mitotic
1087 spindle. **(E)** Sister chromatids segregate to opposite spindle poles during anaphase and **(F)** form
1088 interphase nuclei after cytokinesis. **(G)** A two-cell embryo with both cells undergoing anaphase. **(H)**
1089 A four-cell stage embryo with all cells in interphase. **(I-P)** Hybrid embryos derived from *C.*
1090 *nouraguensis* (NIC59) female x *C. becei* (QG711) crosses. **(I-L)** Hybrid embryos that do not exhibit

1091 abnormalities in centrosome inheritance or pronuclear decondensation and migration **(M-P)** Hybrid
1092 embryos that exhibit abnormalities during early embryogenesis. **(M)** Centrosomes in hybrid
1093 embryos can be dissociated from the male pronucleus during pronuclear migration. Both pronuclei
1094 are condensed. **(N)** A one-cell hybrid embryo with misaligned DNA at metaphase (arrowhead). **(O)**
1095 A two-cell hybrid embryo with lagging DNA between the two interphase cells (arrowhead). **(P)** A
1096 two-cell hybrid embryo during interphase. One cell has an extra smaller nucleus (micronucleus,
1097 arrowhead). **(Q)** Quantification of embryos with abnormalities like those shown in Fig 6M-P.

1098

1099 **Fig 7. Diploid maternal inheritance can occur independently of interspecies hybridization.**
1100 **(A)** Flowchart illustrating how the UV irradiation experiments were conducted. **(B)** A DNA gel
1101 showing the chromosome I genotypes (oPL181+182) of several rare viable F1 derived from
1102 crossing either *C. nouraguensis* JU1825 females to UV-irradiated *C. nouraguensis* NIC59 males
1103 (J♀ x N♂ UV) or NIC59 females to UV-irradiated JU1825 males (N♀ x J♂ UV). The sex of the rare
1104 viable F1 is depicted above each lane, with an identifying number as subscript. **(C)** A DNA gel
1105 showing the chromosome III and V genotypes (oPL78+79 and oPL356+357) of the rare F1 from
1106 Fig 7B that had a maternal genotype for chromosome I. All also had a maternal genotype at these
1107 two markers. **(D)** A table quantifying the frequency of gynogenetically-produced offspring from all
1108 *C. nouraguensis* intraspecies UV experiments (two for each cross). **(E)** A table quantifying the
1109 number of DAPI staining bodies in the -1 oocytes of gynogenetically-produced females from *C.*
1110 *nouraguensis* intraspecies UV experiments. **(F)** A two-cell embryo derived from an intraspecies *C.*
1111 *nouraguensis* cross (JU1825♀ x NIC59♂). Two polar bodies are indicated by white arrowheads.
1112 White lines outline cells. Scale bar: 20 μm. **(G)** A two-cell embryo derived from an intraspecies *C.*
1113 *nouraguensis* cross with irradiated males (JU1825♀ x NIC59♂ UV). Two polar bodies are indicated
1114 by white arrowheads. Lagging DNA (likely UV-irradiated paternal DNA) is indicated by the white
1115 arrow. **(H)** Quantification of polar bodies in *C. nouraguensis* intraspecies crosses.

1116

1117 **Fig 8. Models for diploid maternal inheritance and paternal genome loss in *C. nouraguensis***
1118 **oocytes. (A)** Schematic of canonical meiotic divisions in *C. elegans*. Upon fertilization, each
1119 maternal bivalent (only one shown here) randomly bi-orients its homologs on the meiotic spindle,
1120 cohesion is lost between homologous chromosomes and homologs segregate. One set of
1121 homologs segregates into the first polar body while the other is retained in the oocyte (Anaphase I
1122 and Cytokinesis). Then the half-bivalent in the oocyte randomly bi-orients on the meiotic spindle,
1123 sister chromatid cohesion is lost and sister chromatids segregate. One sister chromatid is
1124 segregated into the second polar body while the other is retained in the oocyte (Anaphase II and
1125 Cytokinesis). Thus, the oocyte inherits only one random chromatid from each bivalent. **(B)** One
1126 model for how female meiosis could be modified to inherit two random homologous chromatids
1127 from a bivalent. Upon fertilization, the bivalent randomly bi-orients its homologs on the meiotic
1128 spindle and cohesion is lost between homologous chromosomes as is normal. Homologs
1129 segregate but cytokinesis fails (Anaphase I) and both half-bivalents remain in the oocyte. Each
1130 half-bivalent then bi-orients on the meiotic spindle, sister chromatid cohesion is lost, and sister
1131 chromatids segregate. One chromatid from each half-bivalent segregates into the second polar
1132 body while the other is retained in the oocyte (Anaphase II and Cytokinesis). Thus, the oocyte
1133 inherits two random homologous chromatids from a bivalent. **(C)** Model of paternal genome loss in
1134 hybrids between *C. nouraguensis* females and *C. becei* males. In nearly all cases, a diploid egg is
1135 produced, but the fate of the embryo depends on the outcome of paternal genome elimination. In
1136 the rare viable offspring the entire haploid *C. becei* paternal genome except for the X chromosome
1137 is inherited in all cells (sterile triploid hybrids), only a subset of cells (sterile diploid-triploid mosaic
1138 hybrids), or in no cells (fertile asexually-produced offspring). The vast majority of the offspring are
1139 dead embryos that have partial losses of the paternal genome in at least some cells and are

1140 aneuploid. Approximately half of the dead embryos inherit the *C. becei* X chromosome that is toxic
1141 to hybrids.

1142 **REFERENCES**

1143

1144 1. Felsenstein J. THE EVOLUTIONARY ADVANTAGE OF RECOMBINATION. Genetics.
1145 1976;78: 737–756. doi:S1090-0233(10)00296-0 [pii]\r10.1016/j.tvjl.2010.09.005 [doi]
1146 2. Gibson AK, Delph LF, Lively CM. The two-fold cost of sex: Experimental evidence from a
1147 natural system. Evol Lett. 2017;1: 6–15. doi:10.1002/evl3.1
1148 3. Maynard Smith J. What use is sex? J Theor Biol. 1971;30: 319–335. doi:10.1016/0022-
1149 5193(71)90058-0
1150 4. Dacks J, Roger AJ. The First Sexual Lineage and the Relevance of Facultative Sex. J Mol
1151 Evol. 1999;48: 779–83.
1152 5. Kassir Y, Granot D, Simchen G. IME1, a Positive Regulator Gene of Meiosis in S. cerevisiae.
1153 Cell. 1988;52: 853–862.
1154 6. Bell G. The masterpiece of nature□: the evolution and genetics of sexuality. University of
1155 California Press, Berkeley CA; 1982.
1156 7. Burke NW, Bonduriansky R. Sexual Conflict, Facultative Asexuality, and the True Paradox of
1157 Sex. Trends in Ecology and Evolution. Elsevier Ltd; 2017. pp. 646–652.
1158 doi:10.1016/j.tree.2017.06.002
1159 8. Mirzaghaderi G, Hörandl E. The evolution of meiotic sex and its alternatives. Proc R Soc B
1160 Biol Sci. 2016;283: 20161221. doi:10.1098/rspb.2016.1221
1161 9. Beukeboom LW, Vrijenhoek RC. Evolutionary genetics and ecology of sperm-dependent
1162 parthenogenesis. J Evol Biol. 1998;11: 755–782. doi:10.1007/s000360050117
1163 10. Coyne JA, Orr HA. Speciation. Sunderland, MA: Sinauer Associates; 2004.
1164 11. Dobzhansky T. On the sterility of the interracial hybrids in Drosophila pseudoobscura. Proc
1165 Natl Acad Natl Acad Sci. 1933;19: 397–403. doi:10.1073/pnas.19.4.397
1166 12. Gibeaux R, Acker R, Kitaoka M, Georgiou G, van Kruijsbergen I, Ford B, et al. Paternal

1167 chromosome loss and metabolic crisis contribute to hybrid inviability in Xenopus. Nature.
1168 2018;553: 337–341. doi:10.1038/nature25188
1169 13. Sanei M, Pickering R, Kumke K, Nasuda S, Houben A. Loss of centromeric histone H3
1170 (CENH3) from centromeres precedes uniparental chromosome elimination in interspecific
1171 barley hybrids. Proc Natl Acad Sci. 2011;108: E498–E505. doi:10.1073/pnas.1103190108
1172 14. Ferree PM, Barbash DA. Species-specific heterochromatin prevents mitotic chromosome
1173 segregation to cause hybrid lethality in Drosophila. PLoS Biol. 2009;7: e1000234.
1174 doi:10.1371/journal.pbio.1000234
1175 15. Vrijenhoek RC. Genetic and ecological constraints on the origins and establishment of
1176 unisexual vertebrates. Evol Ecol Unisexual Vertebr. 1989; 24–31.
1177 16. Avise JC. Clonality: The Genetics, Ecology, and Evolution of Sexual Abstinence in
1178 Vertebrate Animals. Oxford University Press; 2009.
1179 doi:10.1093/acprof:oso/9780195369670.001.0001
1180 17. Lehtonen J, Schmidt DJ, Heubel K, Kokko H. Evolutionary and ecological implications of
1181 sexual parasitism. Trends Ecol Evol. 2013;28: 297–306. doi:10.1016/j.tree.2012.12.006
1182 18. Newton AA, Schnittker RR, Yu Z, Munday SS, Baumann DP, Neaves WB, et al. Widespread
1183 failure to complete meiosis does not impair fecundity in parthenogenetic whiptail lizards.
1184 Development. 2016;143: 4486–4494. doi:10.1242/dev.141283
1185 19. Ting JJ, Woodruff GC, Leung G, Shin N-R, Cutter AD, Haag ES. Intense sperm-mediated
1186 sexual conflict promotes reproductive isolation in Caenorhabditis nematodes. PLoS Biol.
1187 2014;12: e1001915. doi:10.1371/journal.pbio.1001915
1188 20. Sadler PL, Shakes DC. Anucleate Caenorhabditis elegans sperm can crawl, fertilize oocytes
1189 and direct anterior-posterior polarization of the 1-cell embryo. Development. 2000;127: 355–
1190 366.
1191 21. Cutter AD, Dey A, Murray RL. Evolution of the Caenorhabditis elegans genome. Mol Biol

1192 Evol. 2009;26: 1199–1234. doi:10.1093/molbev/msp048
1193 22. Roelens B, Schvarzstein M, Villeneuve AM. Manipulation of karyotype in Caenorhabditis
1194 elegans reveals multiple inputs driving pairwise chromosome synapsis during meiosis.
1195 Genetics. 2015;201: 1363–1379. doi:10.1534/genetics.115.182279
1196 23. Fierst JL, Willis JH, Thomas CG, Wang W, Reynolds RM, Ahearne TE, et al. Reproductive
1197 Mode and the Evolution of Genome Size and Structure in Caenorhabditis Nematodes. PLoS
1198 Genet. 2015;11: e1005323. doi:10.1371/journal.pgen.1005323
1199 24. Meneely PM, Farago AF, Kauffman TM. Crossover distribution and high interference for both
1200 the X chromosome and an autosome during oogenesis and spermatogenesis in
1201 Caenorhabditis elegans. Genetics. 2002;162: 1169–1177.
1202 25. Madl JE, Herman RK. POLYPLOIDS AND SEX DETERMINATION IN CAENORHABDITIS
1203 ELEGANS. Genetics. 1979;93: 393–402.
1204 26. Rockman M V., Kruglyak L. Recombinational landscape and population genomics of
1205 Caenorhabditis elegans. PLoS Genet. 2009;5: e1000419. doi:10.1371/journal.pgen.1000419
1206 27. Ross JA, Koboldt DC, Staisch JE, Chamberlin HM, Gupta BP, Miller RD, et al.
1207 Caenorhabditis briggsae recombinant inbred line genotypes reveal inter-strain incompatibility
1208 and the evolution of recombination. PLoS Genet. 2011;7: e1002174.
1209 doi:10.1371/journal.pgen.1002174
1210 28. Oegema K, Hyman AA. Cell division. WormBook, ed C elegans Res Community, Wormb.
1211 doi:10.1895/wormbook.1.72.1
1212 29. Itono M, Okabayashi N, Morishima K, Fujimoto T, Yoshikawa H, Yamaha E, et al. Cytological
1213 Mechanisms of Gynogenesis and Sperm Incorporation in Unreduced Diploid Eggs of the
1214 Clonal Loach, Misgurnus anguillicaudatus (Teleostei: Cobitidae). J Exp Zool. 2007;307A:
1215 35–50. doi:10.1002/jez.a
1216 30. Grosmaire M, Launay C, Siegwald M, Brugière T, Estrada-Virrueta L, Berger D, et al. Males

1217 as somatic investment in a parthenogenetic nematode. Science. 2019;363: 1210–1213.
1218 doi:10.1126/science.aau0099
1219 31. Fopp-Bayat D, Ocalewicz K, Kucinski M, Jankun M, Laczynska B. Disturbances in the ploidy
1220 level in the gynogenetic sterlet Acipenser ruthenus. J Appl Genet. 2017;58: 373–380.
1221 doi:10.1007/s13353-017-0389-2
1222 32. Goda T, Abu-Daya A, Carruthers S, Clark MD, Stemple DL, Zimmerman LB. Genetic
1223 screens for mutations affecting development of Xenopus tropicalis. PLoS Genet. 2006;2:
1224 e91. doi:10.1371/journal.pgen.0020091
1225 33. Hiruta C, Nishida C, Tochinai S. Abortive meiosis in the oogenesis of parthenogenetic
1226 Daphnia pulex. Chromosom Res. 2010;18: 833–840. doi:10.1007/s10577-010-9159-2
1227 34. Severson AF, Ling L, van Zuylen V, Meyer BJ. The axial element protein HTP-3 promotes
1228 cohesin loading and meiotic axis assembly in C. elegans to implement the meiotic program
1229 of chromosome segregation. Genes Dev. 2009;23: 1763–1778. doi:10.1101/gad.1808809
1230 35. McNally KP, Panzica MT, Kim T, Cortes DB, McNally FJ. A novel chromosome segregation
1231 mechanism during female meiosis. Mol Biol Cell. 2016;27: 2576–2589.
1232 doi:10.1091/mbc.E16-05-0331
1233 36. Murdy WH, Carson HL. Parthenogenesis in Drosophila mangabeirai Malog. Am Nat.
1234 1959;93: 355–363. doi:10.1086/282095
1235 37. Cutter AD, Baird SE, Charlesworth D. High nucleotide polymorphism and rapid decay of
1236 linkage disequilibrium in wild populations of Caenorhabditis remanei. Genetics. 2006;174:
1237 901–913. doi:10.1534/genetics.106.061879
1238 38. Dey A, Chan CKW, Thomas CG, Cutter AD. Molecular hyperdiversity defines populations of
1239 the nematode Caenorhabditis brenneri. Proc Natl Acad Sci U S A. 2013;110: 11056–60.
1240 doi:10.1073/pnas.1303057110
1241 39. Jaquiéry J, Stoeckel S, Larose C, Nouhaud P, Rispe C, Mieuzet L, et al. Genetic Control of

1242 Contagious Asexuality in the Pea Aphid. PLoS Genet. 2014;10: e1004838.
1243 doi:10.1371/journal.pgen.1004838
1244 40. Lamatsch DK, Schmid M, Schartl M. A somatic mosaic of the gynogenetic Amazon molly. J
1245 Fish Biol. 2002;60: 1417–1422. doi:10.1006/jfbi.2002.1939
1246 41. Goddard KA, Megwinoff O, Wessner LL, Giaimo F. Confirmation of gynogenesis in Phoxinus
1247 eos-neogaeus (Pisces: Cyprinidae). J Hered. 1998;89: 151–157.
1248 doi:10.1093/jhered/89.2.151
1249 42. Aldrich JC, Leibholz A, Cheema MS, Ausió J, Ferree PM. A “selfish” B chromosome induces
1250 genome elimination by disrupting the histone code in the jewel wasp Nasonia vitripennis. Sci
1251 Rep. 2017;7: 42551. doi:10.1038/srep42551
1252 43. Werren JH, Baldo L, Clark ME. Wolbachia: master manipulators of invertebrate biology. Nat
1253 Rev Microbiol. 2008;6: 741–751. doi:10.1038/nrmicro1969
1254 44. Yamaki T, Yasuda GK, Wakimoto BT. The deadbeat paternal effect of uncapped sperm
1255 telomeres on cell cycle progression and chromosome behavior in Drosophila melanogaster.
1256 Genetics. 2016;203: 799–816. doi:10.1534/genetics.115.182436
1257 45. Yasuda GK, Schubiger G, Wakimoto BT. Genetic Characterization of ms(3) K81, a paternal
1258 effect gene of Drosophila melanogaster. Genetics. 1995;140: 219–229.
1259 46. Nelson-Rees WA, Hoy MA, Roush RT. Heterochromatinization, chromatin elimination and
1260 haploidization in the parahaploid mite Metaseiulus occidentalis (Nesbitt) (Acarina:
1261 Phytoseiidae). Chromosoma. 1980;77: 263–276. doi:10.1007/BF00286052
1262 47. Baker BS. PATERNAL LOSS (PAL): A MEIOTIC MUTANT IN DROSOPHILA
1263 MELANOGASTER CAUSING LOSS OF PATERNAL CHROMOSOMES. Genetics. 1975;80:
1264 267–96.
1265 48. Kiontke KC, Félix M-A, Ailion M, Rockman M V., Braendle C, Pénigault J-B, et al. A
1266 phylogeny and molecular barcodes for Caenorhabditis, with numerous new species from

1267 rotting fruits. BMC Evol Biol. 2011;11: 339. doi:10.1186/1471-2148-11-339
1268 49. Stevens L, Félix M-A, Beltran T, Braendle C, Caurcel C, Fausett S, et al. Comparative
1269 genomics of 10 new *Caenorhabditis* species. Evol Lett. 2019; 3: 217-236. doi:
1270 10.1002/evl3.110
1271 50. Brenner S. The Genetics of Caenorhabditis elegans. Genetics. 1974;77: 71–94.
1272 doi:10.1111/j.1749-6632.1999.tb07894.x
1273 51. Edgar RC. MUSCLE: Multiple sequence alignment with high accuracy and high throughput.
1274 Nucleic Acids Res. 2004;32: 1792–1797. doi:10.1093/nar/gkh340
1275 52. Guindon S, Dufayard J-F, Lefort V, Anisimova M, Hordijk W, Gascuel O. New algorithms and
1276 methods to estimate maximum-likelihood phylogenies: Assessing the performance of PhyML
1277 3.0. Syst Biol. 2010;59: 307–321. doi:10.1093/sysbio/syq010
1278 53. Lamelza P, Ailion M. Cytoplasmic–Nuclear Incompatibility Between Wild Isolates of
1279 Caenorhabditis nouraguensis. G3. 2017;7: 823–834. doi:10.1534/g3.116.037101
1280 54. Collins TJ. ImageJ for microscopy. Biotechniques. 2007;43: S25–S30.
1281 doi:10.2144/000112505
1282 55. Palopoli MF, Rockman M V., TinMaung A, Ramsay C, Curwen S, Aduna A, et al. Molecular
1283 basis of the copulatory plug polymorphism in Caenorhabditis elegans. Nature. 2008;454:
1284 1019–1022. doi:10.1038/nature07171
1285 56. Robinson JT, Thorvaldsdóttir H, Winckler W, Guttman M, Lander ES, Getz G, et al.
1286 Integrative genomics viewer. Nat Biotechnol. 2011;29: 24–26. doi:10.1038/nbt.1754
1287 57. Bhalla N, Dernburg AF. A conserved checkpoint monitors meiotic chromosome synapsis in
1288 Caenorhabditis elegans. Science. 2005;310: 1683–6. doi:10.1126/science.1117468
1289 58. Sunnucks P, Hales DF. Numerous transposed sequences of mitochondrial cytochrome
1290 oxidase I-II in aphids of the genus Sitobion (Hemiptera: Aphididae). Mol Biol Evol. 1996;13:
1291 510–524.

1292 59. Leggett RM, Clavijo BJ, Clissold L, Clark MD, Caccamo M. NextClip: an analysis and read
1293 preparation tool for Nextera Long Mate Pair libraries. Bioinformatics. 2014;30: 566–568.
1294 60. Davis MPA, van Dongen S, Abreu-Goodger C, Bartonicek N, Enright AJ. Kraken: A set of
1295 tools for quality control and analysis of high-throughput sequence data. Methods. 2013;63:
1296 41–49.
1297 61. Greenfield P, Duesing K, Papanicolaou A, Bauer DC. Blue: correcting sequencing errors
1298 using consensus and context. Bioinformatics. 2014;30: 2723–2732.
1299 62. Simpson JT, Durbin R. Efficient de novo assembly of large genomes using compressed data
1300 structures. Genome Res. 2012;22: 549–56.
1301 63. English AC, Richards S, Han Y, Wang M, Vee V, Qu J, et al. Mind the Gap: Upgrading
1302 Genomes with Pacific Biosciences RS Long-Read Sequencing Technology. Liu Z, editor.
1303 PLoS One. 2012;7: e47768. doi:10.1371/journal.pone.0047768
1304 64. Hunt M, Kikuchi T, Sanders M, Newbold C, Berriman M, Otto TD. REAPR: a universal tool
1305 for genome assembly evaluation. Genome Biol. 2013;14: R47. doi:10.1155/2013/108486
1306 65. Li H, Durbin R. Fast and accurate long-read alignment with Burrows–Wheeler transform.
1307 Bioinformatics. 2010;26: 589–595. doi:10.1093/bioinformatics/btp698
1308 66. McKenna A, Hanna M, Banks E, Sivachenko A, Cibulskis K, Kernytsky A, et al. The Genome
1309 Analysis Toolkit: A MapReduce framework for analyzing next-generation DNA sequencing
1310 data. Genome Res. 2010;20: 1297–1303. doi:10.1101/gr.107524.110.20
1311 67. Kajitani R, Toshimoto K, Noguchi H, Toyoda A, Ogura Y, Okuno M, et al. Efficient de novo
1312 assembly of highly heterozygous genomes from whole-genome shotgun short reads.
1313 Genome Res. 2013;24: 1384–1395. doi:10.1038/nbt.2727
1314 68. Kurtz S, Phillippy A, Delcher AL, Smoot M, Shumway M, Antonescu C, et al. Versatile and
1315 open software for comparing large genomes. Genome Biol. 2004;5: R12.
1316 69. Andolfatto P, Davison D, Erezyilmaz D, Hu TT, Mast J, Sunayama-Morita T, et al.

1317 Multiplexed shotgun genotyping for rapid and efficient genetic mapping. Genome Res.
1318 2011;21: 610–7. doi:10.1101/gr.115402.110
1319 70. Broman KW, Wu H, Sen S, Churchill GA. R/qtl: QTL mapping in experimental crosses.
1320 Bioinformatics. 2003;19: 889–890. doi:10.1093/bioinformatics/btg112
1321 71. Taylor J, Butler D. R Package ASMap: Efficient Genetic Linkage Map Construction and
1322 Diagnosis. J Stat Softw. 2017;79: 1–29. doi:10.18637/jss.v079.i06
1323 72. Kent WJ, Baertsch R, Hinrichs A, Miller W, Haussler D. Evolution's cauldron: duplication,
1324 deletion, and rearrangement in the mouse and human genomes. Proc Natl Acad Sci U S A.
1325 2003;100: 11484–9. doi:10.1073/pnas.1932072100
1326 73. Laetsch DR, Blaxter ML. BlobTools: Interrogation of genome assemblies. F1000Research.
1327 2017;6: 1287. doi:10.12688/f1000research.12232.1
1328 74. Wu TD, Nacu S. Fast and SNP-tolerant detection of complex variants and splicing in short
1329 reads. Bioinformatics. 2010;26: 873–881. doi:10.1093/bioinformatics/btq057
1330 75. Liu Y, Schröder J, Schmidt B. Musket: a multistage k-mer spectrum-based error corrector for
1331 Illumina sequence data. Bioinformatics. 2013;29: 308–315.
1332 doi:10.1093/bioinformatics/bts690
1333 76. Simão FA, Waterhouse RM, Ioannidis P, Kriventseva E V., Zdobnov EM. BUSCO: Assessing
1334 genome assembly and annotation completeness with single-copy orthologs. Bioinformatics.
1335 2015;31: 3210–3212. doi:10.1093/bioinformatics/btv351
1336 77. Hunter SS, Lyon RT, Sarver BAJ, Hardwick K, Forney LJ, Settles ML. Assembly by Reduced
1337 Complexity (ARC): a hybrid approach for targeted assembly of homologous sequences.
1338 bioRxiv. 2015; 014662. doi: 10.1101/014662. doi:10.1101/014662
1339 78. Dey A, Jeon Y, Wang G-X, Cutter AD. Global population genetic structure of Caenorhabditis
1340 remanei reveals incipient speciation. Genetics. 2012;191: 1257–1269.
1341 doi:10.1534/genetics.112.140418

1342 79. Li H, Handsaker B, Wysoker A, Fennell T, Ruan J, Homer N, et al. The Sequence
1343 Alignment/Map format and SAMtools. Bioinformatics. 2009;25: 2078–2079.
1344 doi:10.1093/bioinformatics/btp352
1345 80. Huber W, Carey VJ, Gentleman R, Anders S, Carlson M, Carvalho BS, et al. Orchestrating
1346 high-throughput genomic analysis with Bioconductor. Nat Methods. 2015;12: 115–121.
1347 doi:10.1038/nmeth.3252
1348 81. Olshen AB, Venkatraman ES, Lucito R, Wigler M. Circular binary segmentation for the
1349 analysis of array-based DNA copy number data. Biostatistics. 2004;5: 557–572.
1350 doi:10.1093/biostatistics/kxh008
1351 82. Cutter AD, Jovelin R, Dey A. Molecular hyperdiversity and evolution in very large
1352 populations. Mol Ecol. 2013;22: 2074–2095. doi:10.1111/mec.12281
1353
1354

1355 **SUPPORTING INFORMATION LEGENDS**

1356 **Fig S1. Crosses measuring intra-strain viability and intraspecies and interspecies fecundity.**
1357 **(A)** Wild isolates of *C. becei* (QG704 and QG711) and *C. nouraguensis* (NIC59 and JU1825) have
1358 high levels of intra-strain viability. All strains have a sex ratio skewed towards females, some of
1359 which show a statistically significant difference from a 50:50 sex ratio (Fisher's exact test with
1360 Bonferroni correction, JU1825 p=1.0, NIC59 p=0.06, QG711 p=0.03, QG704 p=0.03). The total
1361 number of offspring quantified for each cross is shown to the right of each bar graph. Data from
1362 both graphs are derived from the same crosses. **(B)** A graph showing the number of embryos laid
1363 for intraspecies *C. nouraguensis* crosses (10 NIC59 females x 10 NIC59 males) and interspecies
1364 *C. nouraguensis* female x *C. becei* male crosses (10 NIC59 females x 10 QG711 males) in a one-
1365 hour window on each of the first three days after the crosses were set. There are three replicates
1366 for each type of cross. Each point represents the number of embryos laid for a replicate in a one-
1367 hour window that day and the bar graph shows the average of those replicates. The *C.*
1368 *nouraguensis* female x *C. becei* male interspecies hybridization had significantly less embryos on
1369 days 2 and 3 of egg-laying as compared to the intraspecies *C. nouraguensis* crosses (*, day 2
1370 p=0.04, day 3 p=0.04, Kruskal-Wallis test).

1371

1372 **Fig S2. Summary of interspecies crosses.** Rows show the females of each cross and males are
1373 shown in columns. The wild isolate strains used for each species are indicated. Black boxes are
1374 intraspecies crosses. Grey boxes are untested interspecies hybridizations. Rare viable F1 adults
1375 are present only when crossing *C. nouraguensis* females to *C. becei* males. Rare viable but sick
1376 F1 larvae are present in both directions of *C. becei* x *C. yunquensis* crosses. Worms mate but do
1377 not produce F1 embryos in *C. panamensis* female x *C. nouraguensis* male and *C. becei* female x
1378 *C. panamensis* male crosses. At least 12,000 dead F1 were screened for each cross that gave
1379 embryos.

1380

1381 **Fig S3. Fertile progeny with a maternal genotype and sterile progeny with a hybrid genotype**
1382 **are produced when *C. nouraguensis* females are crossed to males of a different *C. becei***
1383 ***strain*. (A)** We tested the fertility of rare viable F1 derived from *C. nouraguensis* JU1825 x *C. becei*
1384 QG704 crosses by backcrossing to JU1825 individuals of the opposite sex. F1 were then
1385 genotyped at the ITS2 locus using a PCR-RFLP assay. **(B)** A gel showing the sex, fertility and
1386 genotype at the ITS2 locus of viable adult F1. All fertile F1 have a maternal genotype, with one
1387 exception: one hybrid F1 female laid inviable F2 embryos (F*, still considered fertile). All sterile F1
1388 had a hybrid genotype. **(C)** A table summarizing the genotyping data in (B).

1389

1390 **Fig S4. Fertile F1 females are diploid.** The -1 oocytes from *C. nouraguensis* JU1825 and *C.*
1391 *becei* females primarily have six DAPI- staining bodies (two examples shown here). Most fertile F1
1392 females derived from JU1825 female x QG711 male crosses have six DAPI-staining bodies
1393 (Example fertile F1 female #1). A minority have eight DAPI-staining bodies. In three of these
1394 cases, there appear to be seven relatively normal sized DAPI bodies plus a very small one
1395 (Example fertile F1 female #2, small DAPI body highlighted by white arrowhead). In the other two
1396 cases, all eight DAPI bodies appear roughly equal in size (Example fertile F1 female #3). This
1397 higher number of DAPI-staining bodies is not the chance observation of a low frequency meiotic
1398 defect in a nucleus that happens to be in the -1 oocyte position (for example, homologs fail to
1399 recombine and increase the number of univalents) because we observed the same number of
1400 DAPI-staining bodies in both germlines of the same fertile F1 female. We hypothesize that these
1401 extra DAPI-staining bodies represent extra DNA (either maternal or paternal) in addition to the two
1402 chromatids inherited from each maternal bivalent. Scale bar: 5 μm.

1403

1404 **Fig S5. Fertile F1 inherit two randomly selected homologous chromatids from each**
1405 **maternal bivalent. (A)** The six possible ways of combining two of the four genetically distinct
1406 chromosomes in a bivalent are illustrated, with their expected genotypic signature below them.
1407 There are five distinct genotypic signatures. Two result from combining sister-chromatids and are
1408 called "Sisters_1" and "Sisters_2". Three result from combining homologous chromosomes and
1409 are called "Homologs_1", "Homologs_2" and "Homologs_3". (**B)** A table summarizing the genotype
1410 of each maternal chromosome for each sequenced F1 individual. The F1's sex and fertility are
1411 noted. Each individual's ploidy is inferred from the genotyping data. The genotype
1412 "Homologs_ambiguous" refers to chromosomes that are heterozygous in their centers, but one end
1413 of the chromosome is not obviously heterozygous (N/J) or homozygous for either NIC59 or
1414 JU1825. The genotype "Hemizygous X" refers to hemizygous X-chromosomes in males that have
1415 half the read depth of the autosomes. The genotype "Triploid" refers to chromosomes that have
1416 three copies instead of two based on relative read depth and whole-chromosome genotype. The
1417 "Sisters_3" genotype refers to chromosomes that have inherited two non-recombinant JU1825
1418 chromatids. Three fertile females (F1_8, F1_11 and F1_39) have NIC59 and JU1825 alleles in the
1419 center of their chromosomes, but exhibit a slight skew from the expected 0.50 NIC59 allele
1420 frequency (Fig S7). We hypothesize that this skew is due to contaminating DNA derived from
1421 backcrossing each female when testing her fertility. For example, a viable female that was
1422 backcrossed to a JU1825 male would carry JU1825 sperm and therefore JU1825 DNA in her
1423 spermatheca. In this case, the contaminating DNA would skew the female's entire genome to a
1424 lower NIC59 SNP frequency. Consistent with this, in all three females the more abundant allele
1425 matches the genotype of the male she was backcrossed to (Table S1). Correcting for this potential
1426 backcrossing contamination, the genotypes of all the chromosomes in these three females are
1427 consistent with the inheritance of two homologous chromatids. One fertile female (F1_25) and two
1428 sterile females (F1_18 and F1_26) have a very low proportion of NIC59 reads across their entire

1429 genome (Fig S7). We hypothesize this skew is due to contaminating DNA from JU1825 males
1430 during fertility testing and poor lysis of the female (Table S1). The low proportion of NIC59 reads
1431 made it difficult to infer actual maternal chromosome genotypes and are therefore categorized as
1432 "ambiguous". **(C)** Tables summarizing the frequency of genotypes per chromosome in all fertile F1,
1433 all sterile F1, or a combination of all fertile and sterile F1.
1434
1435 **Fig S6. Genotypic signatures of multiple potential mechanisms of diploid maternal**
1436 **inheritance. (A)** A schematic of the cross used to determine how diploidy is restored in
1437 gynogenetically produced offspring in the interspecies cross. Heterozygous (NIC59/JU1825) *C.*
1438 *nouraguensis* females are crossed to *C. becei* (QG711) males. Individual viable offspring resulting
1439 from the hybridization undergo whole genome sequencing. **(B)** If diploid maternal inheritance
1440 results from mitotic (apomixis) rather than meiotic divisions, then viable F1 are clones of their
1441 mother and will be heterozygous NIC59/JU1825 across their entire genome (0.5 NIC59 allele
1442 frequency). **(C)** Diploid maternal inheritance can occur through endomitosis, which is when a
1443 haploid maternal genome replicates without a cell division. This results in two exact copies of each
1444 chromosome and therefore homozygosity for either NIC59 (1.0 NIC59 allele frequency) or JU1825
1445 alleles (0.0 NIC59 allele frequency) across the entire genome. **(D)** Diploid maternal inheritance can
1446 occur through automixis (combining two of the four meiotic products). Combining two homologous
1447 chromatids will result in heterozygosity in the center of a chromosome, and heterozygosity or
1448 homozygosity at the chromosome ends. Combining two sister chromatids will result in
1449 homozygosity in the center of a chromosome and heterozygosity at one of the ends.
1450 Inheriting two sister chromatids for one chromosome and two homologous chromatids for another
1451 chromosome in the same genome is theoretically possible, but not depicted here.
1452

1453 **Fig S7. Fertile F1 inherit two randomly selected homologous chromatids from each**
1454 **maternal bivalent.** Each of the following pages contains plots describing whole-genome
1455 sequencing data of either a rare viable F1 individual or a control DNA sample. The sample name is
1456 at the top of each page, along with the individual's sex, fertility and strain it was backcrossed to for
1457 fertility testing (if applicable). Each page has five rows of plots. The first row shows the genotypes
1458 of the sample's *C. nouraguensis* maternal chromosomes (i.e. average NIC59 allele frequency in
1459 50-kb windows across the *C. nouraguensis* assembly). Haplotype change points and average
1460 allele frequency for each segment are shown by the green horizontal lines. The second and third
1461 rows show the sample's average read coverage of the *C. becei* and *C. nouraguensis* assemblies in
1462 50-kb windows. The fourth and fifth rows show the average GC content of the *C. becei* and *C.*
1463 *nouraguensis* assemblies in 50-kb windows. The gray vertical lines represent breaks between
1464 scaffolds.
1465
1466 **Fig S8. Fertilization with UV-irradiated sperm does not cause frequent diploid maternal**
1467 **inheritance in intraspecies crosses. (A)** Fertilization with UV-irradiated sperm does not
1468 significantly increase diploid maternal inheritance in *C. nouraguensis* intraspecies crosses.
1469 Heterozygous *C. nouraguensis* (NIC59/JU1825) females were mated to UV-irradiated *C.*
1470 *nouraguensis* (NIC59) males. Dead embryos produced by this cross were PCR genotyped at a
1471 single autosomal locus (oPL78+79). The gel shows the genotypes of a fraction of the dead
1472 embryos assayed. Most embryos had either a JU1825 (11/31) or NIC59 genotype (17/31),
1473 consistent with haploid maternal inheritance and destruction of the paternal NIC59 genome.
1474 Although 3/31 embryos had a heterozygous genotype (red stars), we found that UV-irradiation can
1475 fail to completely destroy the paternal genome (see Fig S8B), suggesting that these three
1476 heterozygotes may result from haploid maternal inheritance of a JU1825 allele and haploid
1477 paternal inheritance of a NIC59 allele due to incomplete destruction of paternal DNA. **(B)** The

1478 paternal genome is not always eliminated by UV irradiation. *C. nouraguensis* (JU1825) females
1479 were mated to UV-irradiated *C. nouraguensis* (NIC59) males. Dead embryos produced by this
1480 cross were PCR genotyped at a single autosomal locus (oPL78+79). The gel shows the genotypes
1481 of a fraction of the dead embryos assayed. Red stars indicate cases in which the UV-irradiated
1482 paternal NIC59 DNA can be detected.
1483
1484 **Table S1. Characteristics of the samples submitted for whole-genome sequencing.** Whole-
1485 genome amplified F1 individuals derived from the interspecies cross are labeled as "F1_" followed
1486 by a barcode number. Sample "F1_NIC59_JU1825" is one heterozygous NIC59/JU1825 female
1487 that was whole-genome amplified and serves as a control for genome-wide heterozygosity.
1488 Sample "NIC59plusJU1825" comprises one NIC59 and one JU1825 female placed in the same
1489 tube and whole-genome amplified. This also serves as a control for genome-wide heterozygosity.
1490 Sample "NIC59plusJU1825plusQG711" comprises one NIC59, one JU1825 and one QG711
1491 female placed into the same tube and whole-genome amplified. This serves as a triploid (diploid *C.*
1492 *nouraguensis* and haploid *C. becei*) control. The "NIC59_bulk", "JU1825_bulk" and "QG711_bulk"
1493 samples are genomic preps made from large populations of each strain containing mixed
1494 developmental stages and sexes: these libraries were prepared without whole-genome
1495 amplification. The reads from the "NIC59_bulk" and "JU1825_bulk" samples were used to identify
1496 fixed SNPs between the two strains. The second column shows the interspecies cross that
1497 produced each viable F1 animal. In each case, heterozygous N/J *C. nouraguensis* females were
1498 crossed to *C. becei* QG711 males. However, the heterozygous *C. nouraguensis* females could
1499 have either a NIC59 or JU1825 mitochondrial genotype (denoted in parentheses). A fraction of
1500 each sample's reads (Illumina 50-bp paired end) derive from *E.coli* (their food). The *E. coli* fraction
1501 is quite high in some samples, likely due to inefficient cleaning of single worms (see Materials and
1502 Methods). Of the reads that map to *Caenorhabditis* nuclear genomes, the approximate coverage

1503 and percent of all worm reads that map to each *Caenorhabditis* nuclear genome are shown.

1504

1505 **Video S1. *C. nouraguensis* (JU1825) embryonic development.** DIC time-lapse imaging of
1506 embryos derived from JU1825 female x JU1825 male crosses. Most develop into larvae, but two
1507 embryos fail to develop. Dissection and mounting of embryos causes some embryos to arrest at
1508 approximately the one-cell stage.

1509

1510 **Video S2. *C. becei* (QG711) embryonic development.** DIC time-lapse imaging of embryos
1511 derived from QG711 female x QG711 male crosses**.** Most develop into larvae, but one embryo fails
1512 to develop. Dissection and mounting of embryos causes some embryos to arrest at approximately
1513 the one-cell stage.

1514

1515 **Video S3. *C. becei* female x *C. nouraguensis* male embryonic death.** DIC time-lapse imaging
1516 of embryos derived from *C. becei* QG711 female x *C. nouraguensis* JU1825 male crosses**.** These
1517 embryos undergo cell divisions until approximately the 32-cell stage at which point they
1518 stereotypically arrest and fail to undergo further divisions. The embryos come out of focus at the
1519 end of the video.

1520

1521 **Video S4. *C. nouraguensis* female x *C. becei* male embryonic death.** DIC time-lapse imaging
1522 of embryos derived from *C. nouraguensis* JU1825 female x *C. becei* QG711 male crosses. These
1523 embryos arrest either at early or later stages of development. The early-arresting embryos
1524 generally have abnormal cell membrane morphologies. Specifically, some arrested embryos have
1525 faint cell membranes that appear to distend and take up more space than the normally more
1526 rounded cells seen in the early embryos of either parental species. Also, some early-arresting
1527 embryos have many nuclei but no discernible cell membranes separating them. The embryos that

1528 arrest at later stages have superficially normal cell and nuclear morphologies and undergo cell
1529 divisions until approximately the 44-87 cell stage. After this point, the cells in these embryos largely
1530 halt their divisions, with many appearing to be dissociated from one another, rounded, and of
1531 variable size. One common feature of the early and late-arresting embryos is that both can have
1532 multinucleate cells.
1533

Fig 1.

A

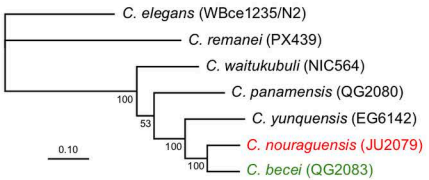

B

cross	viable F1 adults	dead F1 embryos	frequency of viable F1 adults (%)
C. nouraguensis (JU1825) ♀ x *C. becei* (QG711) ♂	5	6239	0.08
C. nouraguensis (NIC59) ♀ x *C. becei* (QG711) ♂	2	5913	0.03
C. nouraguensis (NIC54) ♀ x *C. becei* (QG711) ♂	14	4227	0.33
C. becei (QG711) ♀ x *C. nouraguensis* (JU1825) ♂	0	4530	0
C. becei (QG711) ♀ x *C. nouraguensis* (NIC59) ♂	0	3091	0
C. becei (QG711) ♀ x *C. nouraguensis* (NIC54) ♂	0	4308	0

C

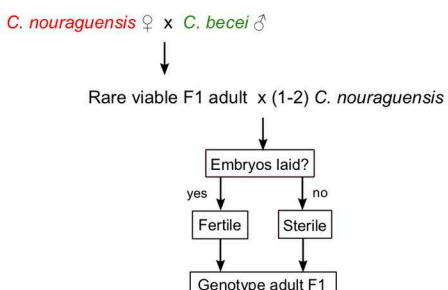

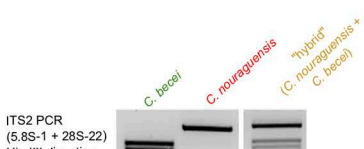

D

C. nouraguensis (JU1825) ♀ x *C. becei* (QG711) ♂

Genotype of F1 adult at W02B12.9 locus (Chr. II)

		Hybrid (*C. nouraguensis*/*C. becei*)		Maternal (*C. nouraguensis*)		
		female	male	female	male	total
Fertility of F1 adult	Fertile	0	0	7	1	8
	Sterile	13	4	1	0	18
	total	13	4	8	1	26

C. nouraguensis (NIC54) ♀ x *C. becei* (QG711) ♂

Genotype of F1 adult at ITS2 locus (Chr. I)

		Hybrid (*C. nouraguensis*/*C. becei*)		Maternal (*C. nouraguensis*)		
		female	male	female	male	total
Fertility of F1 adult	Fertile	0	0	10	0	10
	Sterile	21	5	1	0	27
	total	21	5	11	0	37

Fig 2.

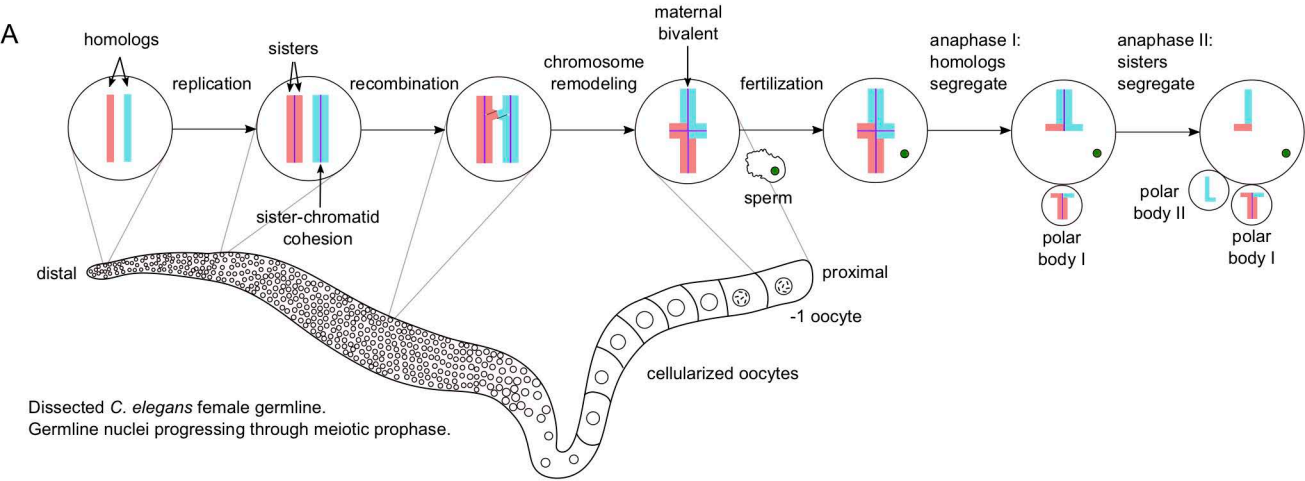
A
homologs
replication
sisters
recombination
chromosome remodeling
maternal bivalent
fertilization
anaphase I: homologs segregate
anaphase II: sisters segregate
sperm
sister-chromatid cohesion
polar body I
polar body II
polar body I
distal
proximal
-1 oocyte
cellularized oocytes
Dissected C. elegans female germline.
Germline nuclei progressing through meiotic prophase.

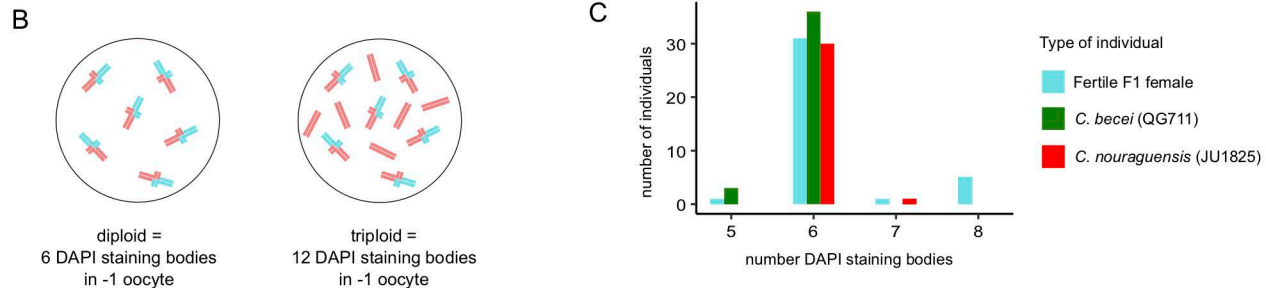
B
diploid =
6 DAPI staining bodies
in -1 oocyte
triploid =
12 DAPI staining bodies
in -1 oocyte
C
number of individuals
0
10
20
30
5
6
7
8
number DAPI staining bodies
Type of individual
Fertile F1 female
C. becei (QG711)
C. nouraguensis (JU1825)

Fig 3.

A

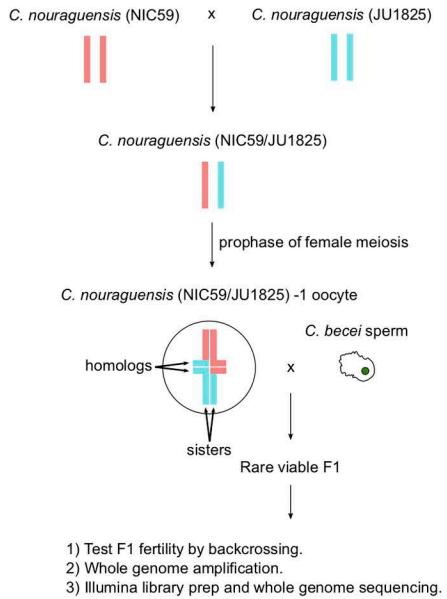

B

C

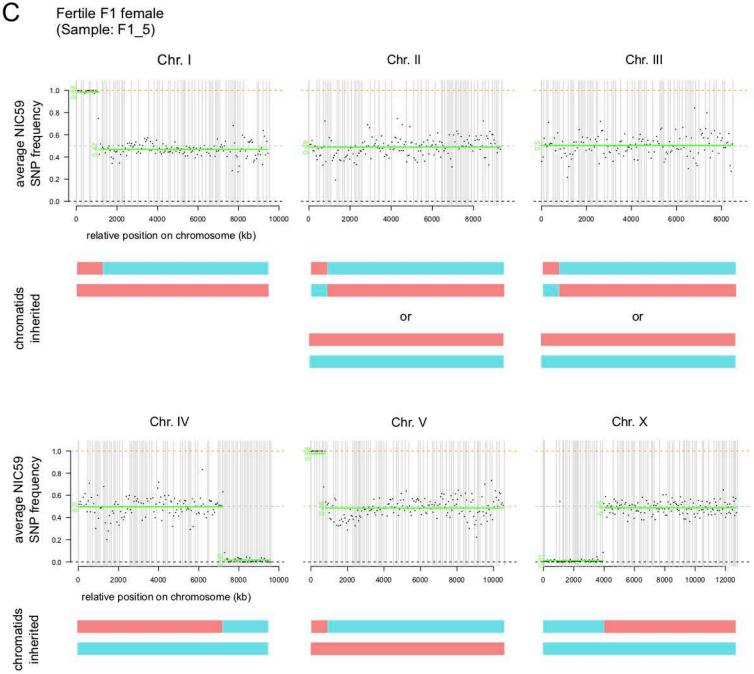

D

	Sisters_1	Sisters_2	Homologs_1	Homologs_2	Homologs_3	total
Observed in combined fertile F1 (10)	0	0	10	10	33	53
Expected if two chromatids randomly inherited	9	9	9	9	18	54
Expected if two homologs randomly inherited	0	0	14	14	28	56

Fig 4.

A

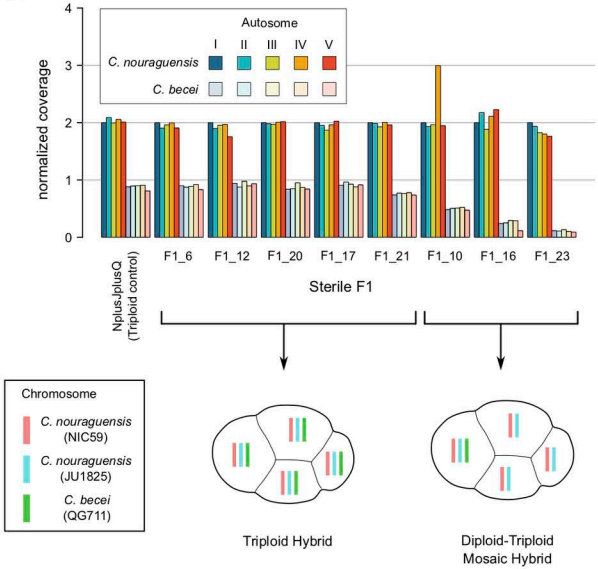

B

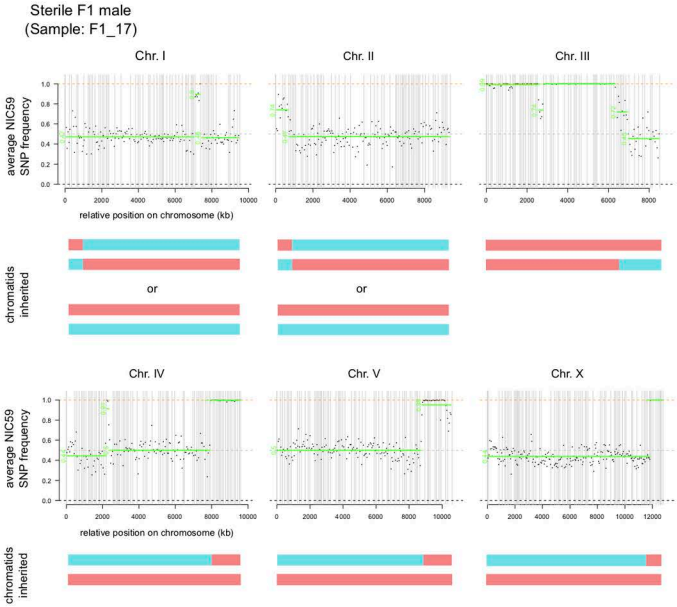

C

	Sisters_1	Sisters_2	Homologs_1	Homologs_2	Homologs_3	total
Observed in combined sterile F1 (8)	1	0	11	13	18	43
Expected if two chromatids randomly inherited	7	7	7	7	14	42
Expected if two homologs randomly inherited	0	0	11	11	22	44

D

	Sisters_1	Sisters_2	Homologs_1	Homologs_2	Homologs_3	total
Observed in combined sterile and fertile F1 (18)	1	0	21	23	51	96
Expected if two chromatids randomly inherited	16	16	16	16	32	96
Expected if two homologs randomly inherited	0	0	24	24	48	96

Fig 5.

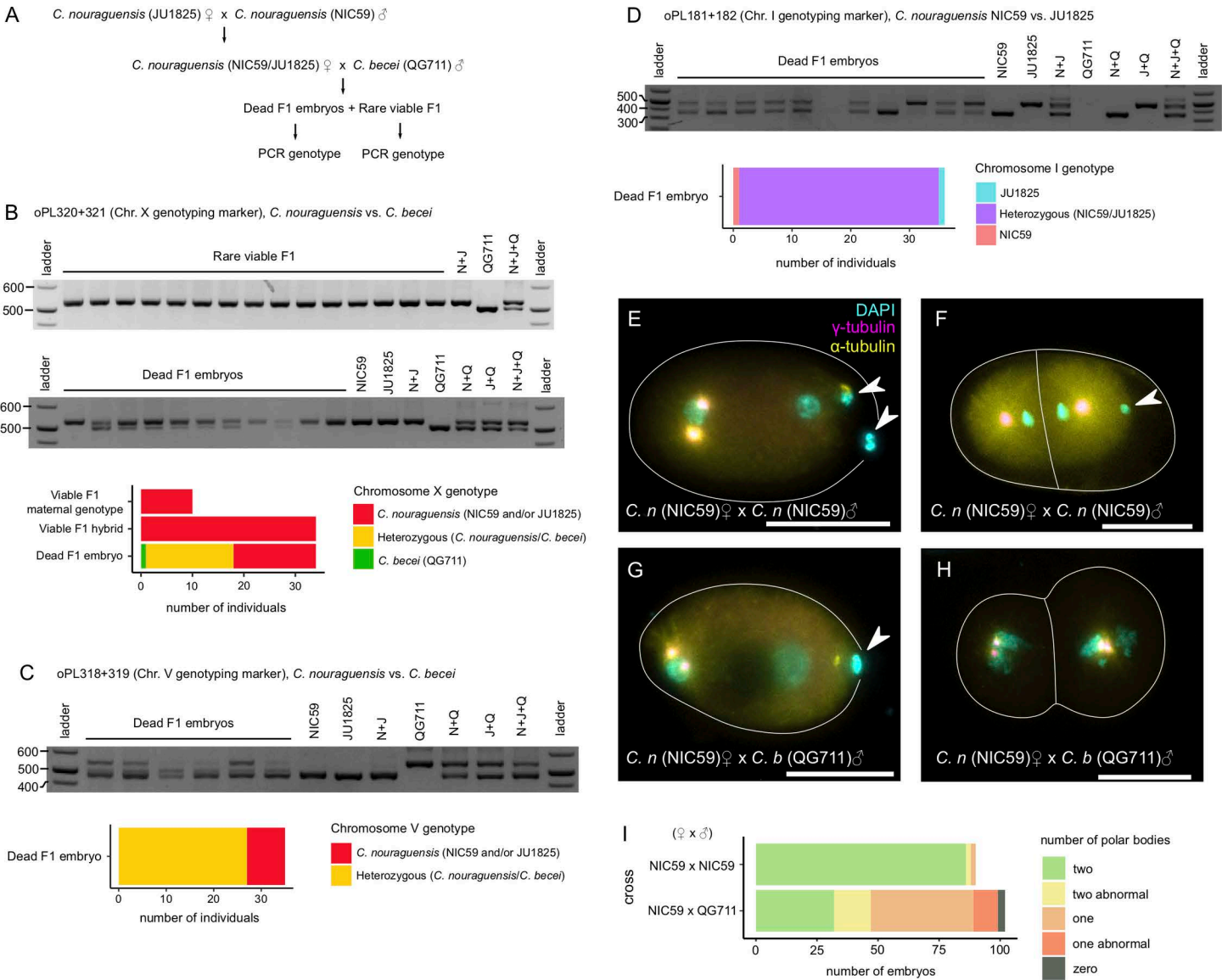
A
C. nouraguensis (JU1825) ♀ x C. nouraguensis (NIC59) ♂
C. nouraguensis (NIC59/JU1825) ♀ x C. becei (QG711) ♂
Dead F1 embryos + Rare viable F1
PCR genotype
PCR genotype
B
oPL320+321 (Chr. X genotyping marker), C. nouraguensis vs. C. becei
ladder
Rare viable F1
N+J
QG711
N+J+Q
ladder
600
500
ladder
Dead F1 embryos
NIC59
JU1825
N+J
QG711
N+Q
J+Q
N+J+Q
ladder
600
500
Viable F1 maternal genotype
Viable F1 hybrid
Dead F1 embryo
0
10
20
30
number of individuals
Chromosome X genotype
C. nouraguensis (NIC59 and/or JU1825)
Heterozygous (C. nouraguensis/C. becei)
C. becei (QG711)
C
oPL318+319 (Chr. V genotyping marker), C. nouraguensis vs. C. becei
ladder
Dead F1 embryos
NIC59
JU1825
N+J
QG711
N+Q
J+Q
N+J+Q
ladder
600
500
400
Dead F1 embryo
0
10
20
30
number of individuals
Chromosome V genotype
C. nouraguensis (NIC59 and/or JU1825)
Heterozygous (C. nouraguensis/C. becei)
D
oPL181+182 (Chr. I genotyping marker), C. nouraguensis NIC59 vs. JU1825
ladder
Dead F1 embryos
NIC59
JU1825
N+J
QG711
N+Q
J+Q
N+J+Q
ladder
500
400
300
Dead F1 embryo
0
10
20
30
number of individuals
Chromosome I genotype
JU1825
Heterozygous (NIC59/JU1825)
NIC59
E
DAPI
γ-tubulin
α-tubulin
C. n (NIC59)♀ x C. n (NIC59)♂
F
C. n (NIC59)♀ x C. n (NIC59)♂
G
C. n (NIC59)♀ x C. b (QG711)♂
H
C. n (NIC59)♀ x C. b (QG711)♂
I
(♀ x ♂)
cross
NIC59 x NIC59
NIC59 x QG711
0
25
50
75
100
number of embryos
number of polar bodies
two
two abnormal
one
one abnormal
zero

Figure 6

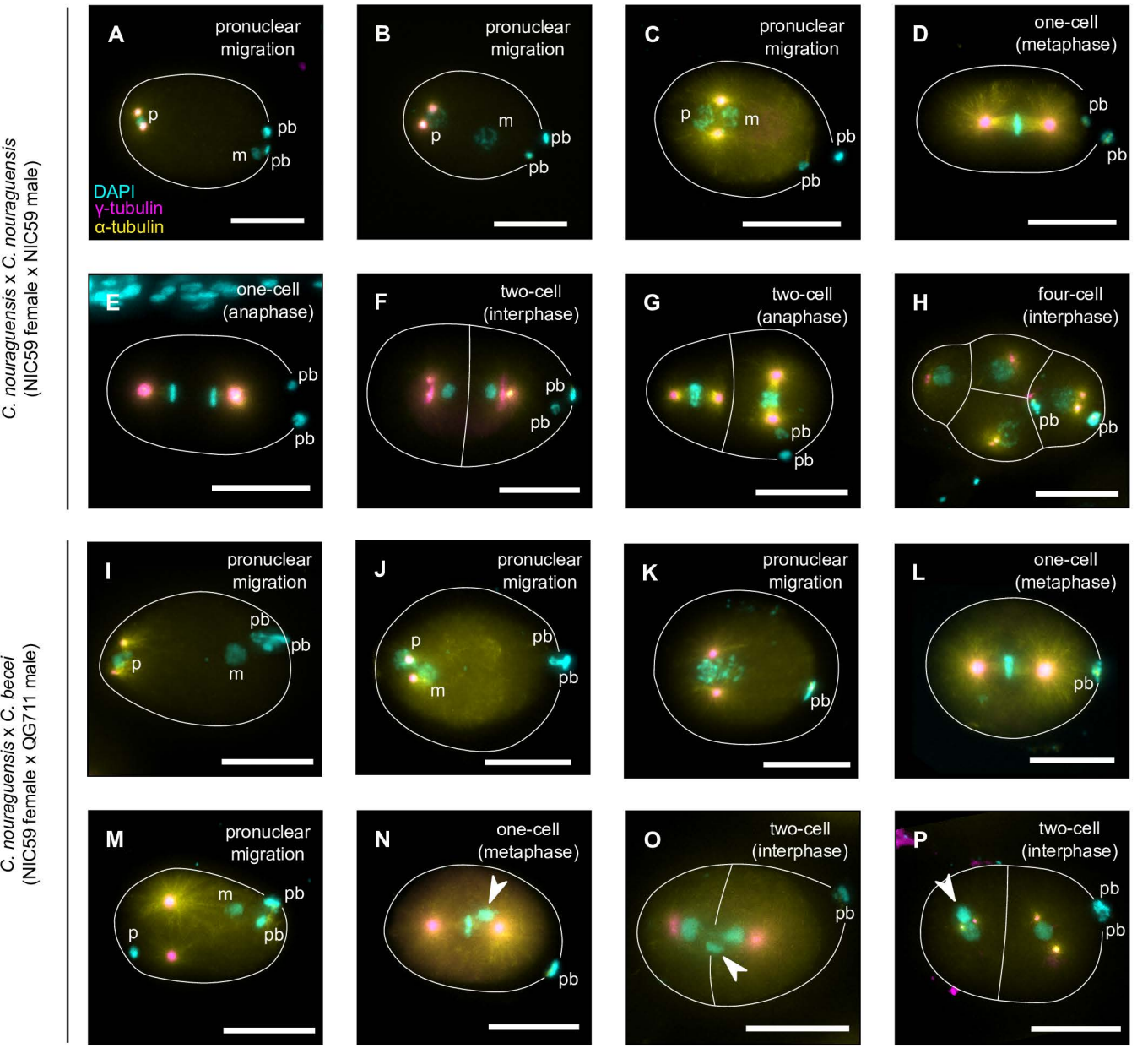
C. nouraguensis x C. nouraguensis
(NIC59 female x NIC59 male)
C. nouraguensis x C. becei
(NIC59 female x QG711 male)
A
pronuclear migration
p
pb
m
pb
DAPI
γ-tubulin
α-tubulin
B
pronuclear migration
m
p
pb
pb
C
pronuclear migration
p
m
pb
pb
D
one-cell (metaphase)
pb
pb
E
one-cell (anaphase)
pb
pb
F
two-cell (interphase)
pb
pb
G
two-cell (anaphase)
pb
pb
H
four-cell (interphase)
pb
pb
I
pronuclear migration
pb
pb
p
m
J
pronuclear migration
p
pb
m
pb
K
pronuclear migration
pb
L
one-cell (metaphase)
pb
M
pronuclear migration
m
pb
p
pb
N
one-cell (metaphase)
pb
O
two-cell (interphase)
pb
P
two-cell (interphase)
pb
pb

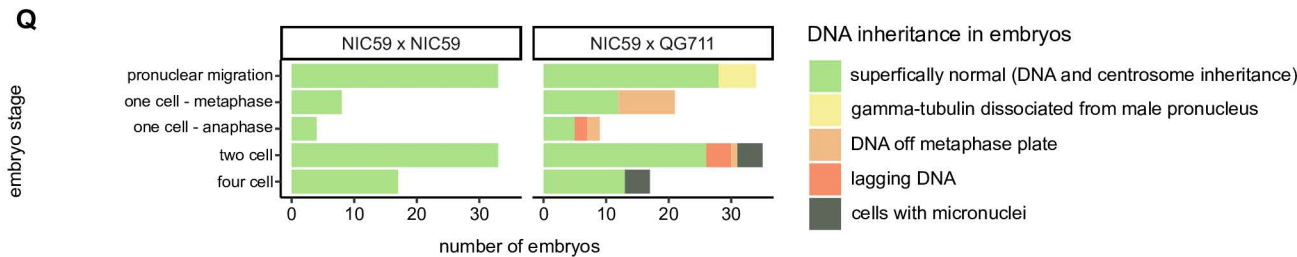
Q
NIC59 x NIC59
NIC59 x QG711
embryo stage
pronuclear migration
one cell - metaphase
one cell - anaphase
two cell
four cell
0
10
20
30
number of embryos
DNA inheritance in embryos
superfically normal (DNA and centrosome inheritance)
gamma-tubulin dissociated from male pronucleus
DNA off metaphase plate
lagging DNA
cells with micronuclei

Fig 7.

A

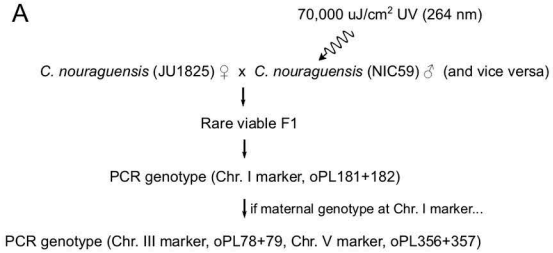

B

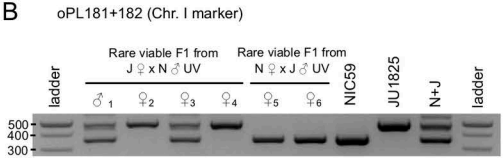

C

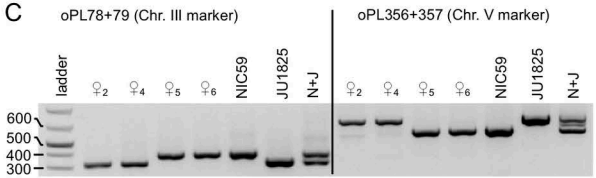

D

cross	Viable F1 w/ maternal genotype at oPL78+79		dead F1 embryos	frequency of gynogenetic offspring (%)
	female	male		
JU1825 ♀ x NIC59 ♂ UV	4	1	~45,000	~0.01
NIC59 ♀ x JU1825 ♂ UV	19	1	~16,000	~0.1

E

-1 oocytes dissected from	# DAPI staining bodies		
	five	six	seven
NIC59 females	2	16	0
Rare F1 females from NIC59 ♀ x JU1825 ♂ UV crosses	3	25	1

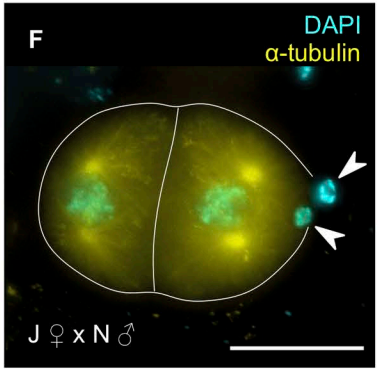

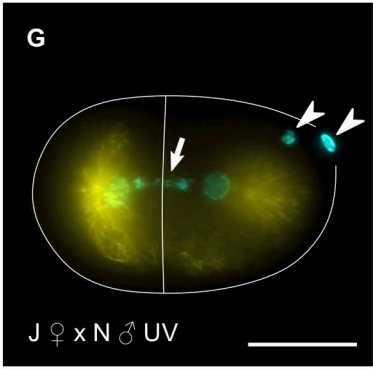

H

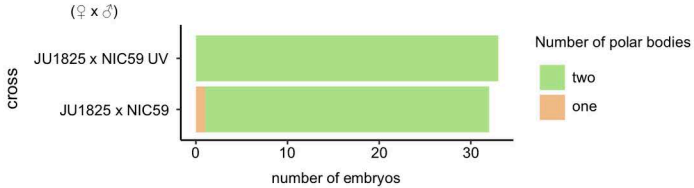

Figure 8

A Normal female meiosis in *C. elegans*

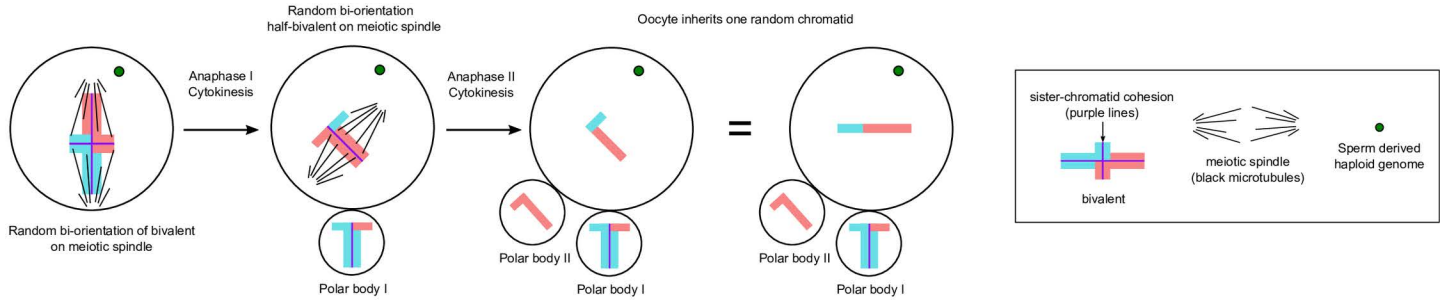

B Model of diploid maternal inheritance

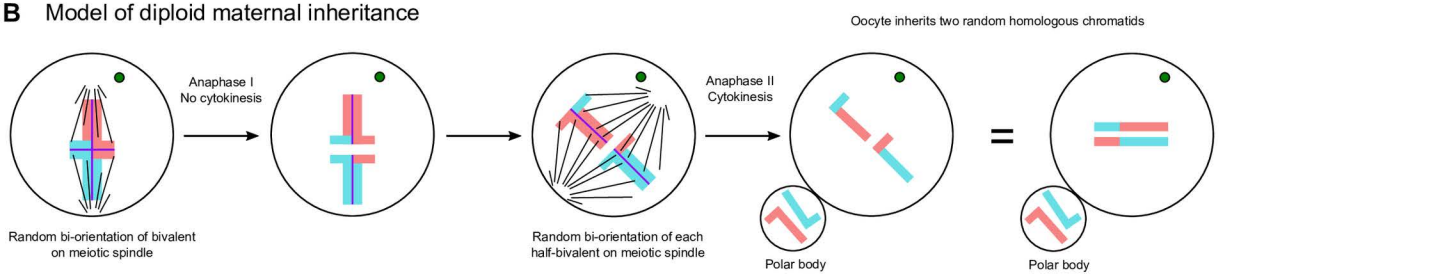
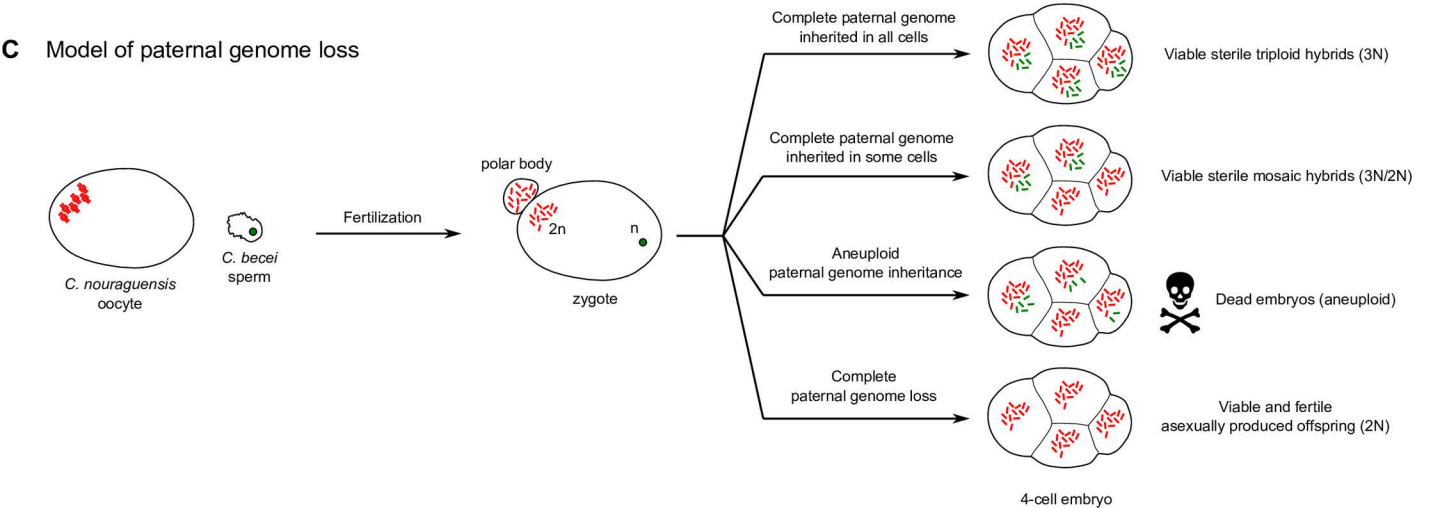
C Model of paternal genome loss